NASA CONTRACTOR

REPORT

NASA CR – 132646

DESIGN AND FABRICATION OF RENE' 41 ADVANCED STRUCTURAL PANELS

By
Bruce E. Greene and Russell F. Northrup

THE BOEING COMPANY

Prepared For

NATIONAL AERONAUTICS AND SPACE ADMINISTRATION

NASA Langley Research Center
Contract NAS1-10749
John L. Shideler Project Manager

NASA CR – 132646

DESIGN AND FABRICATION OF RENE' 41 ADVANCED STRUCTURAL PANELS

By

Bruce E. Greene and Russell F. Northrup

THE BOEING COMPANY

Prepared For

NATIONAL AERONAUTICS AND SPACE ADMINISTRATION

NASA Langley Research Center

Contract NAS1-10749

FOREWORD

This report was prepared by the Boeing Aerospace Company, a division of The Boeing Company, Seattle, Washington for the Langley Research Center of the National Aeronautics and Space Administration. The design and fabrication of advanced tubular structural element and panel test specimens from René 41 material is presented. Test results for the structural element specimens are presented and compared with analytical strength predictions. Predicted strengths for the panel specimens under proposed future test load conditions at elevated temperature are also presented. The work is part of a comprehensive program to develop advanced beaded and tubular structural panel designs and static strength prediction methods under contract NAS1-10749, "Design and Testing of Advanced Structural Panels." This program was under the cognizance of the contract monitor John L. Shideler, reporting to Herman L. Bohon, head of the Thermal Protection Section of the Structures and Dynamics Division, NASA Langley Research Center.

The technical leader and principal investigator on this program was Bruce E. Greene, reporting to the program manager, John L. Arnquist, Chief of the Structural Methods and Allowables organization. Manufacturing activities were under the direction of Russell F. Northrop.

This report was prepared by Bruce E. Greene and Russell F. Northrop in cooperation with John L. Shideler.

The art work and drafts for this report were prepared by Gary A. Jensen.

ABSTRACT

A study was conducted to exploit the efficiency of curved elements in the design of lightweight structural panels under combined loads of axial compression, inplane shear, and bending. A summary of the initial program, which encompassed the design, analysis, fabrication, and test of aluminum panels, is presented in document NASA CR-2514.

The report presented herein describes the application of technology generated in the initial aluminum program to the design and fabrication of René 41 panels for subsequent performance tests at elevated temperature. Optimum designs for two panel configurations are presented. The designs are applicable to hypersonic airplane wing structure and are designed specifically for testing at elevated temperature in the hypersonic wing test structure located at the NASA Flight Research Center. Fabrication methods developed to produce the René panels are described. Test results of smaller structural element specimens are presented to verify the design and fabrication methods used. Predicted strengths of the panels under several proposed elevated temperature test load conditions are presented.

TABLE OF CONTENTS

LIST OF FIGURES

SUMMARY

For several years the Langley Research Center has been investigating structural concepts which use curved elements to develop corrugated, beaded and tubular structural panels. The curved sections exhibit high local buckling strengths which lead to highly efficient structural concepts, and their corrugated nature allows controlled thermal growth to minimize thermal stresses in high temperature applications.

As part of this continuing investigation design methods and fabrication techniques for producing several potentially efficient panel concepts were developed. Room temperature tests of aluminum panels verified that the analytically predicted high structural efficiencies of these panels could be achieved. A summary of this initial work is reported in NASA CR-2514.

The work presented in this report extends the technology developed for aluminum to the design and fabrication of René 41 panels. Governing analytical static strength and stability equations and geometric constraint equations were incorporated in a random search type optimization computer code to identify minimum mass designs for two tubular panel configurations. Fabrication techniques suitable for producing these panel configurations in René 41 material were developed. The principal difference between the aluminum and René 41 assembly techniques was that the aluminum panels were bonded but the René 41 panels were resistance welded. Room temperature buckling tests were conducted on structural element specimens of the two panel designs to verify the design and fabrication methods used. These tests demonstrated adequate strength in the detailed design and fabrication of the end closures to transmit full design and test loads into the structural panels. As a result of these tests one of the configurations was selected for full scale panel fabrication. Six 43 inch x 19 inch (109 cm x 48 cm) panel specimens of this configuration were manufactured and delivered to NASA Flight Research Center where they will be tested at elevated temperature in the hypersonic wing test structure to evaluate their performance.

INTRODUCTION

For several years the Langley Research Center has been investigating structural concepts which use elements with curved cross sections to develop beaded or corrugated skin panel structure (see ref. 1-6). The curved sections exhibit high local buckling strengths which lead to highly efficient structural concepts. These concepts can be applied where a lightly beaded external surface is aerodynamically acceptable or where the structure is not exposed to airflow. Their corrugated nature makes them especially attractive for high temperature application because the controlled thermal growth minimizes thermal stress.

As a part of this continuing program, The Boeing Company under contract NAS1-10749 (see ref. 6-10) has developed the design and fabrication techniques for lightweight structural panels. Under this contract a random search-type computer program was used to identify minimum mass designs for several potentially efficient panel concepts. These panels were designed for combined loads of axial compression, inplane shear, and bending due to lateral pressure. A fabrication technique was developed which has been shown to be cost effective and still permit mass production of panels. Room temperature buckling tests were conducted on aluminum panels built from these concepts to obtain failure data for correlation with theory. These experimental data indicate that the analytically predicted high structural efficiencies of the advanced panel can be achieved.

The work presented herein constitutes the next step in the program, which is to apply the technology generated with aluminum to the design and fabrication of panels in a superalloy material for subsequent performance tests at elevated temperature. The material selected for this work was René 41. Using the analysis methods and computer codes developed in the initial aluminum panel phase, two optimum panel designs were obtained, one for a circular arc tubular configuration, the other for a fluted tubular configuration. The panels were designed to be tested in a realistic hypersonic wing test structure (see ref. 11) located at the NASA Flight Research Center.

The basic fabrication technique developed for aluminum panels was extended and applied to the fabrication of René 41 panels. This extension included development of tooling and forming sequences to produce the parts for the two René 41 panel designs, and the development of a satisfactory welding procedure for joining the parts into completed panel assemblies.

Prior to fabricating the hypersonic wing test panels for delivery to NASA-FRC, smaller size end closure/local buckling specimens of the two designs were fabricated and tested to demonstrate adequate strength in the end closures to transmit panel design and test loads, and to verify the design and analysis methods as applied to the fabricated René 41 panels. As a result of these tests, the circular arc tubular design was selected for full size panel fabrication and testing. Six 43 inch x 19 inch (109 cm x 48 cm) panels of this design were fabricated and delivered to the Flight Research Center where they will be tested at high temperature to evaluate their performance in a typical hypersonic airframe application.

SYMBOLS

E	Modulus of elasticity
F_c	Compression stress at failure
F_{cy}	Compression yield stress
F_s	Shear stress at failure
G	Shear modulus
L	Length of panel
N_x	Axial compression load, lb/in (kN/m)
N_{xy}	Shear load, lb/in (kN/m)
p	Lateral pressure load, lb/in^2 (kN/m^2)
R	Radius
t	Thickness
W	Width of panel

PANEL DESIGN

Optimum designs were obtained for each of two different panel configurations: type 2 (tubular panel) and type 2A (fluted tubular panel). The panel designs were obtained by the use of the OPTRAN computer code. This code employs a random search type optimization routine to determine values of the cross section design variables which constitute a panel of minimum mass per unit area subject to specified load conditions, geometric constraints, and failure mode constraints. The use of OPTRAN to obtain minimum mass panel designs is discussed in reference 8. Analysis equations used to define failure mode constraints for general instability, local instability, and material strength of beaded and tubular panels are also given in reference 8.

Design Conditions

The panel design load conditions were selected to be compatible with the NASA-FRC hypersonic wing test structure, and included combined axial compression, shear, and lateral pressure. Panel design loads were:

$$N_x = 800 \text{ lb/in} \quad (140 \text{ kN/m})$$

$$N_{xy} = 250 \text{ lb/in} \quad (43.8 \text{ kN/m})$$

$$p = 0.75 \text{ lb/in}^2 \quad (5.2 \text{ kN/m}^2)$$

The nominal panel dimensions for design purposes were assumed to be:

$$L = 43 \text{ in} \quad (109 \text{ cm})$$

$$W = 19 \text{ in} \quad (48 \text{ cm})$$

The material properties for René 41 at the design temperature of 1350°F (1005 K) were:

$$E = 23.5 \times 10^6 \text{ lb/in}^2 \quad (162 \text{ GN/m}^2)$$

$$G = 9.04 \times 10^6 \text{ lb/in}^2 \quad (62.3 \text{ GN/m}^2)$$

$$F_{cy} = 101 \times 10^3 \text{ lb/in}^2 \quad (696 \text{ MN/m}^2)$$

Optimum Panel Designs

The final panel cross section designs derived from OPTRAN with the preceding design conditions are shown in figure 1. Each of these designs was taken from the best of four independent OPTRAN runs to insure that the random search technique resulted in a valid optimum design. The designs were constrained to obtain an integral number of tubes within the prescribed panel width. Both designs were also constrained by a minimum material gage of 0.016 in. (0.041 cm).

Figures 2 and 3 show planform and profile details for the two panel types. A clearance of 0.15 in (0.38 cm) was provided in addition to the specified edge margin of 1.10 in (2.79 cm) at each side of the panel. The additional clearance was provided to accommodate the bend radii at the bead mold lines and possible cumulative error in the overall beaded width of the brake-formed panels. The type 2A configuration was also constrained by a minimum flat width of 1.00 in (2.54 cm) to insure adequate width for attaching stand-off clips to support heat shields. The heat shield support locations are shown projected on the planform views in figures 2 and 3.

The OPTRAN design of the type 2 configuration was obtained using the modified failure mode analysis equations which achieved correlation within 5 percent between analysis and test of type 2 aluminum panels, as presented in reference 8. Because of complex modal behavior involving distortions of the fluted tube cross section an acceptable correlation of analysis with test of the type 2A aluminum panels was not achieved. However, preliminary tests indicated that with inserts to stabilize the tube cross-section, an adequate margin of safety could be achieved in the proposed type 2A design.

Panel End Closures

End closure designs for the René 41 panels are shown in figures 2 and 3. These designs were derived from the experience gained in developing satisfactory end closures for tubular aluminum panels. A summary of the aluminum panel end closure development is contained in reference 9.

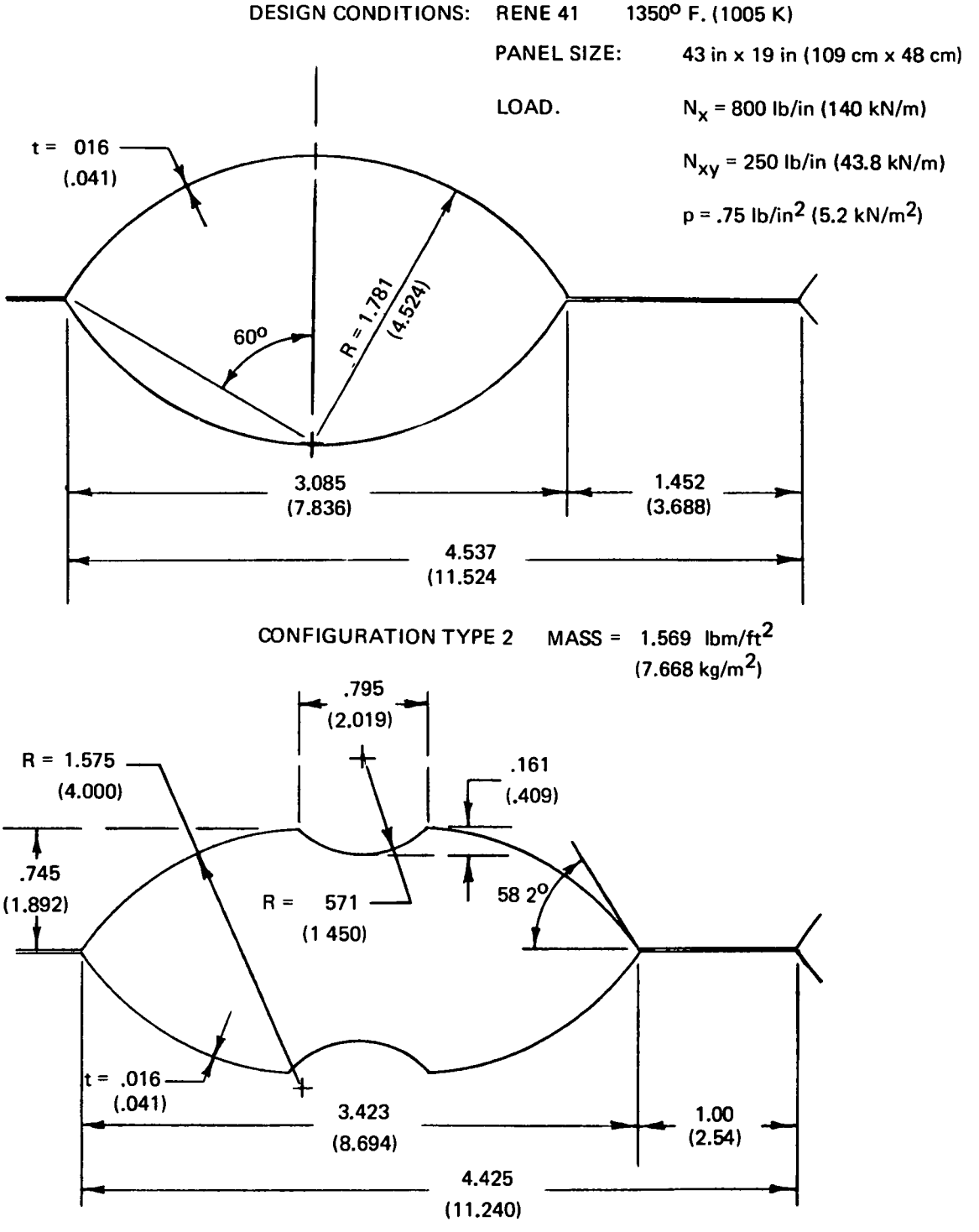

Figure 1. OPTIMUM PANEL CROSS SECTIONS

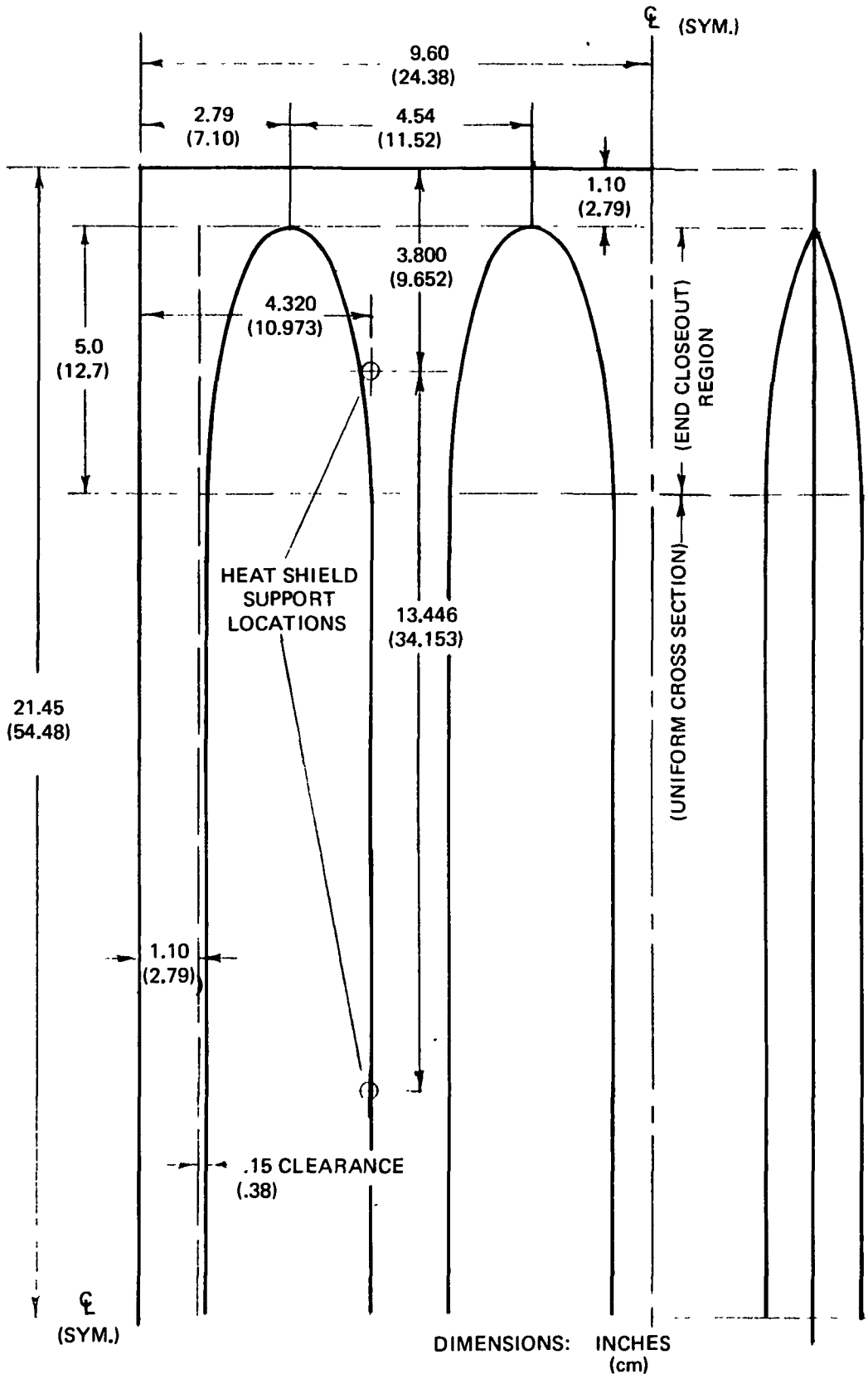

Figure 2. PANEL PLANFORM AND PROFILE DETAILS–CONFIGURATION TYPE 2

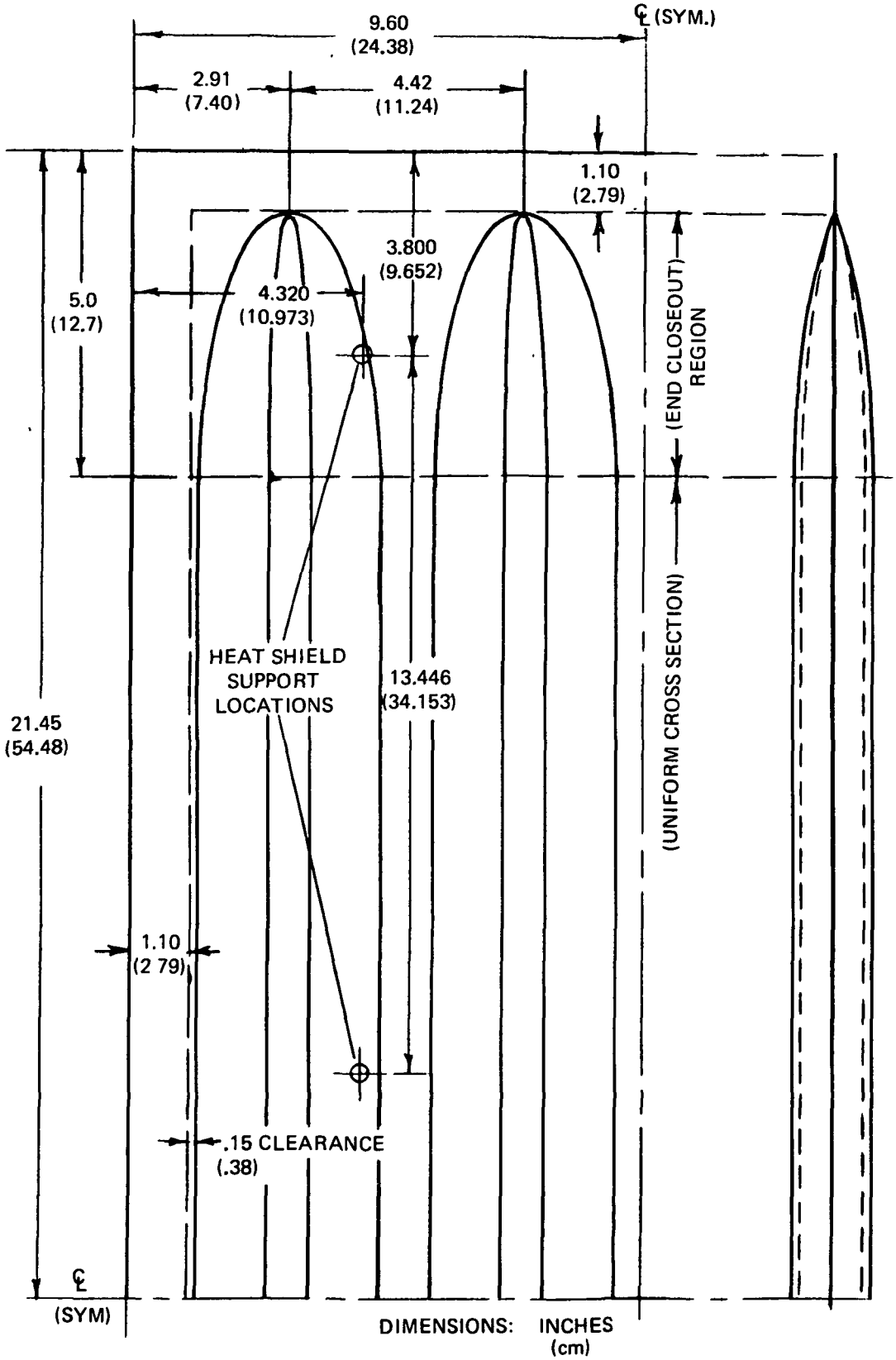

Figure 3. PANEL PLANFORM AND PROFILE DETAILS–CONFIGURATION TYPE 2A

The secondary beads formed in the end closure flat areas during the end closure forming operation are removed prior to final panel assembly. The purpose of forming these secondary beads is to take up the excess width of material in the end closure, thereby preventing compression wrinkling in the flats during forming. The removal of the secondary beads is necessary for two reasons: first, to prevent air flow through the panel, since center sheet doublers which sealed this leakage path in the bonded aluminum panels are not compatible with the welded assembly process used for the René 41 panels; second, to permit a more satisfactory attachment of heat shield support clips.

Doublers

Fingered doublers are required at the panel ends to transmit loads from the flat ends into the beaded portion of the panel. The doublers also serve to stabilize the flat areas in the end closure region. The center sheet doublers which were used successfully with the bonded assembly of the aluminum panels (See ref. 9.) are not feasible with the welded assembly of the René 41 panels. Therefore, the present panel designs call for external doublers only. Figures 4 and 5 show doubler details for the type 2 panel configuration. The doublers consist of two contoured sheets of 0.018 in. (0.046 cm) René 41 material on each surface of the panel at its ends for a total doubler thickness of 0.072 in. (0.183 cm), or 0.036 in. (0.091 cm) on each surface of the panel. This thickness of doubler was selected to match the doubler thickness of the existing beaded panels which these panels will replace in the hypersonic wing test structure described in reference 11. Thus, the tubular panels can be installed directly, without any shimming required to maintain concentric load transfer between the beaded and tubular panels. The 0.036 in. (0.091 cm) doubler thickness will also provide increased stability in the end closure flat areas which is desired with the removal of the secondary beads.

The doubler fingers are tapered to achieve gradual transfer of load into the panel without stress concentrations developing in the flats or the tube walls which might cause premature local buckling. The taper is achieved by stepping from two doubler sheets to one and by planform tapering of the

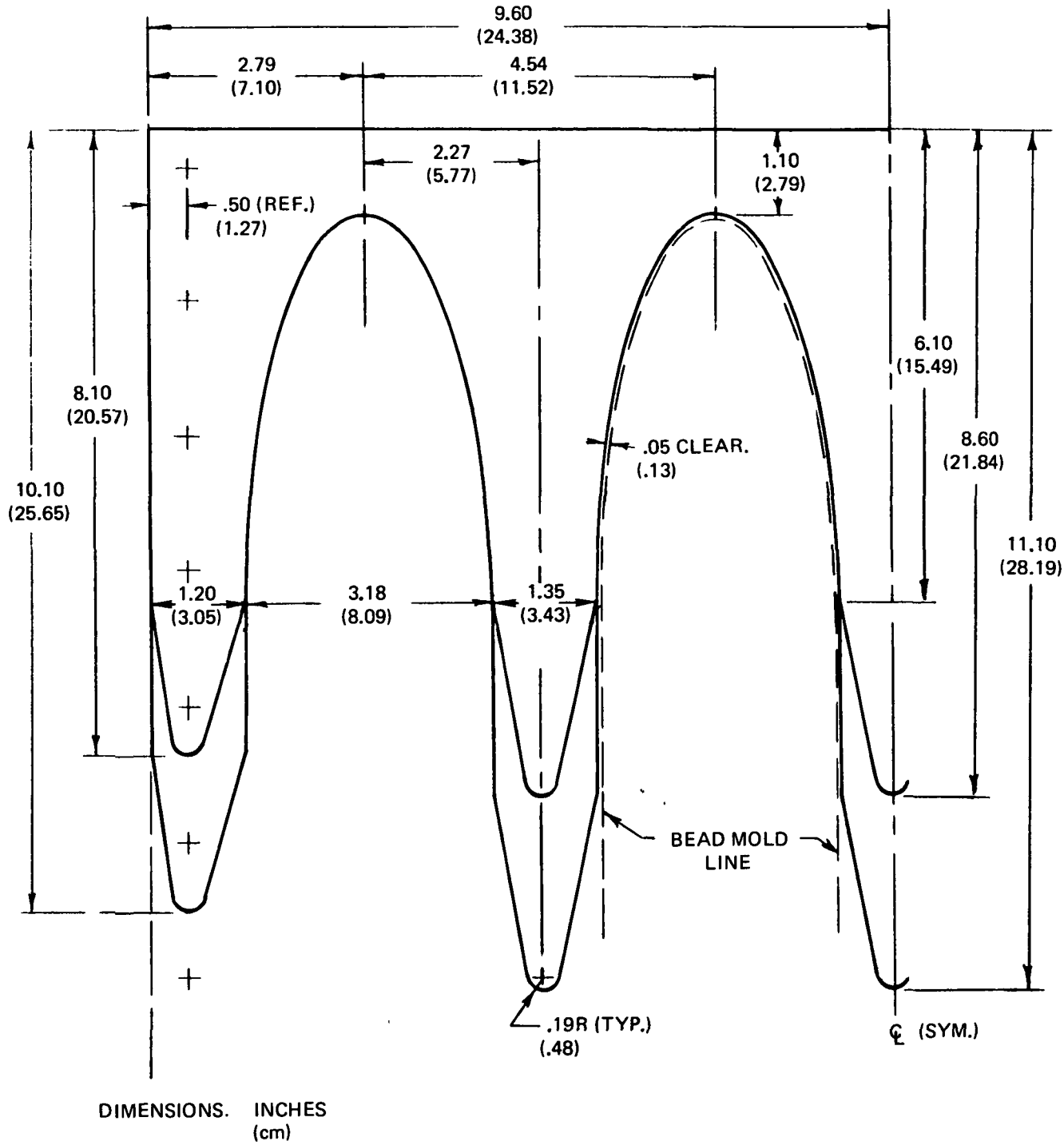

Figure 4. PANEL UPPER SURFACE DOUBLER DETAILS–CONFIGURATION TYPE 2

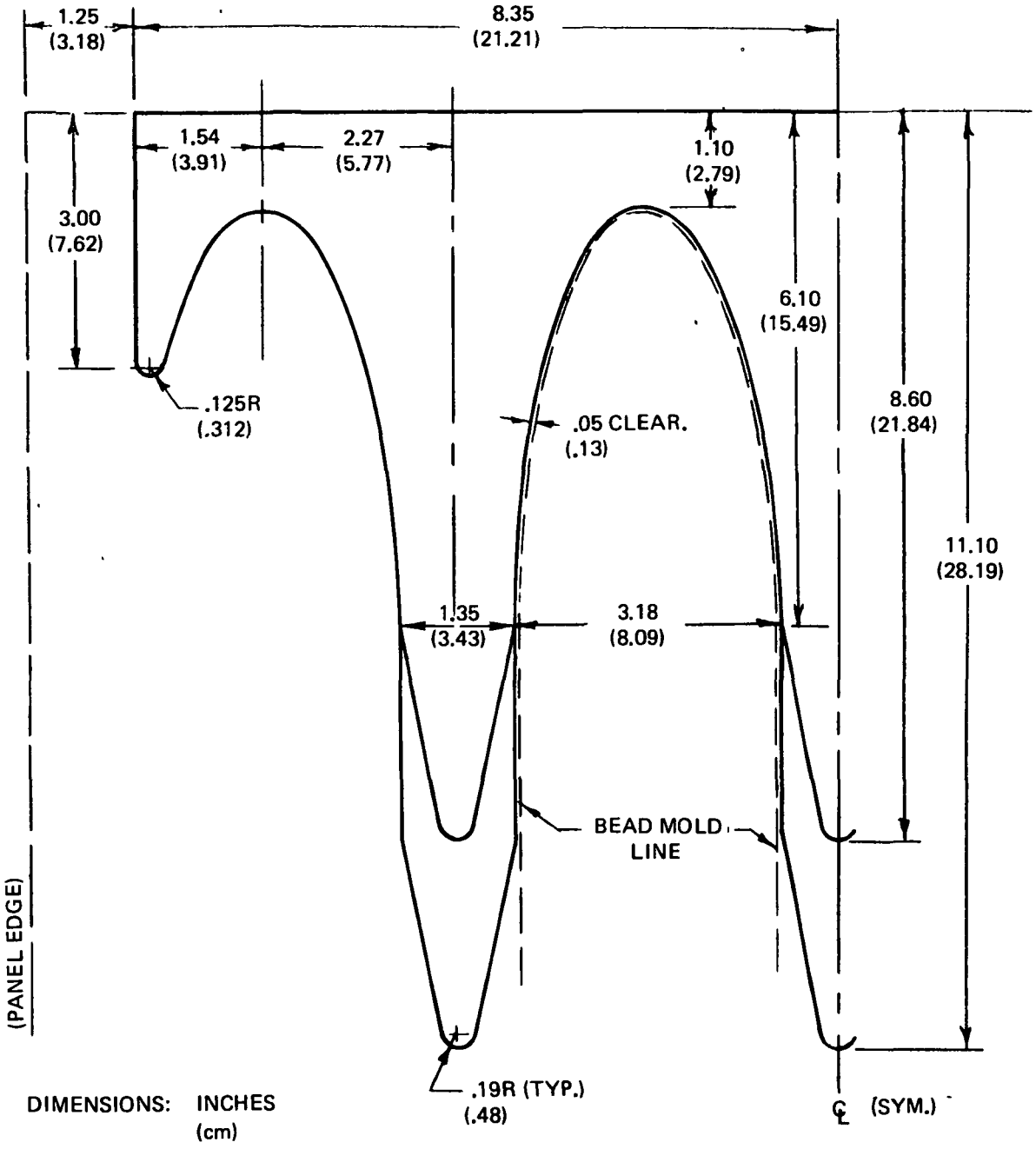

Figure 5. PANEL LOWER SURFACE DOUBLER DETAILS–CONFIGURATION TYPE 2

doubler fingers, as indicated in figures 4 and 5. The planform taper of the doubler fingers was adopted in preference to tapering the thickness because it is difficult to weld multisheet stackups satisfactorily when the outer sheets are appreciably thinner than the interior sheets.

The doubler fingers adjacent to the panel edges have been trimmed away on the lower surface of the panel, i.e., the surface facing the interior of the wing box. This provides clearance for the spar caps to which the panel edges are attached in the same manner as the existing beaded panels. On the upper surface of the panel the lengths of the doubler fingers adjacent to the edges have been tailored so as not to interfere with drilling of the fastener holes. The fastener hole locations along the panel edge are indicated in figure 4.

A nominal clearance of 0.05 in. (0.13 cm) is provided between the doubler planform and the bead mold lines to accommodate bend radii and cumulative error in forming of the beaded sheets.

The doubler details for the type 2A panel configuration are similar to those described for the type 2 panels. The only essential difference is that the doubler fingers are narrower to accommodate the type 2A cross section.

Heat Shield Standoff Clips

Heat shield standoff clips designed for use with the tubular René 41 panels are not necessarily representative of flight hardware. They were designed to hold the heat shields in place during testing in the hypersonic wing test structure. The only design requirement was that they flex sufficiently to allow thermal expansion of the heat shields at 1600°F (1144 K).

The clips are formed from 0.018 in. (0.046 cm) René 41 stock according to the details shown in figure 6. The nut plates (NS103758-02) indicated in the figure are to be furnished and installed by NASA at FRC. The height of the clips is designed to effect a junction with the lower surface of the

heat shield support beams at 1.41 in. (3.58 cm) above the panel mid-plane when the nut plates are installed and the clips are mounted on top of the panel doublers, i.e., at the locations adjacent to the panel ends. When the clips are mounted at the locations adjacent to the panel center, where there are no doublers, they are to be shimmed or bent slightly as necessary to make up the 0.036 in. (0.091 cm) lacking in height, depending on the required tolerances.

The installation of the heat shield clips on the panel is shown in figure 7. The vertical legs of the clips are oriented toward the centers of the heat shield panels to allow unrestricted thermal expansion. Heat shield clips and panels are furnished with mounting holes for No. 10 size fasteners, as indicated in figures 6 and 7.

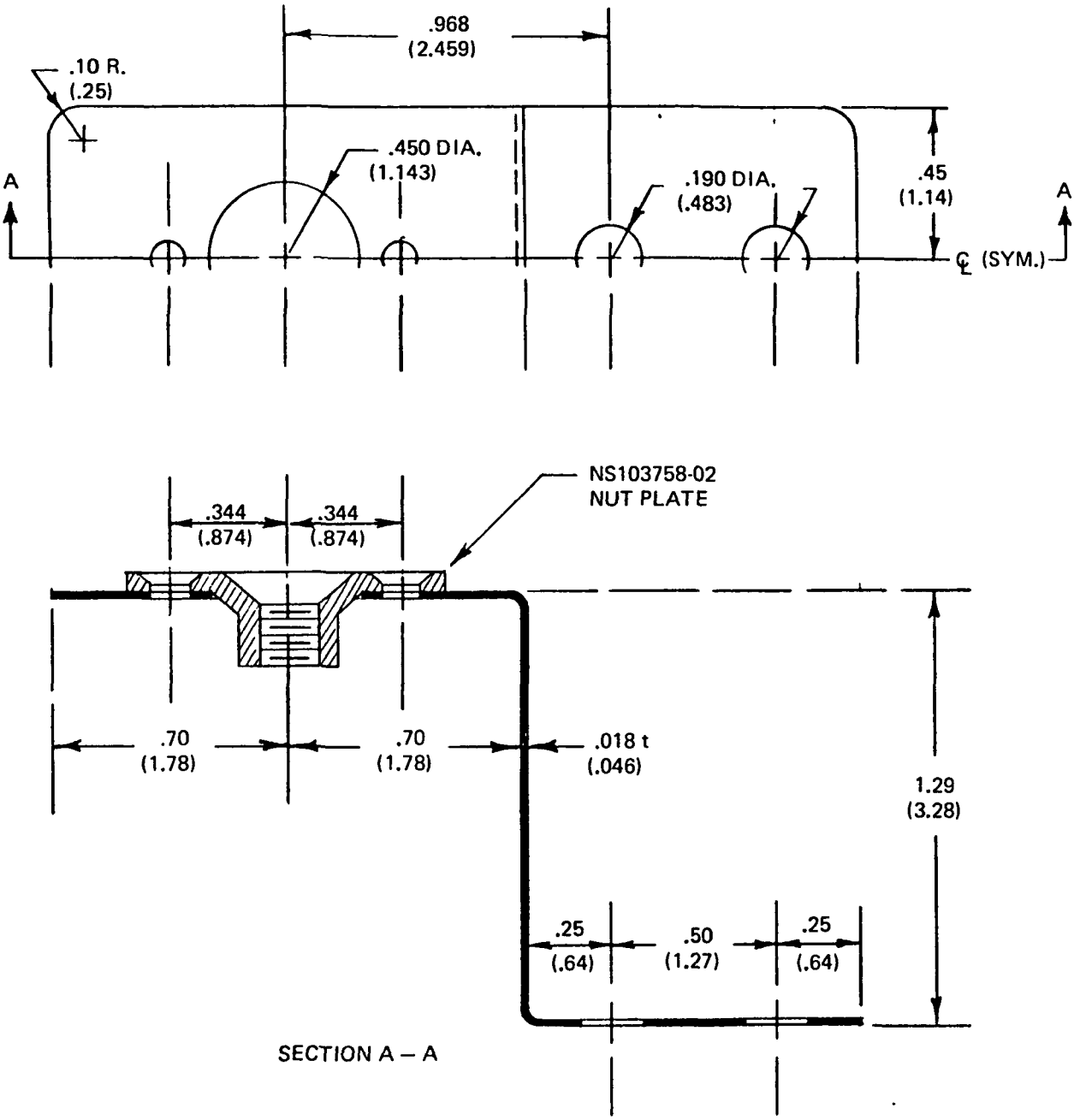

NOTE NUT PLATES TO BE FURNISHED AND INSTALLED BY NASA

DIMENSIONS INCHES (cm)

Figure 6. HEAT SHIELD STANDOFF CLIP DETAIL

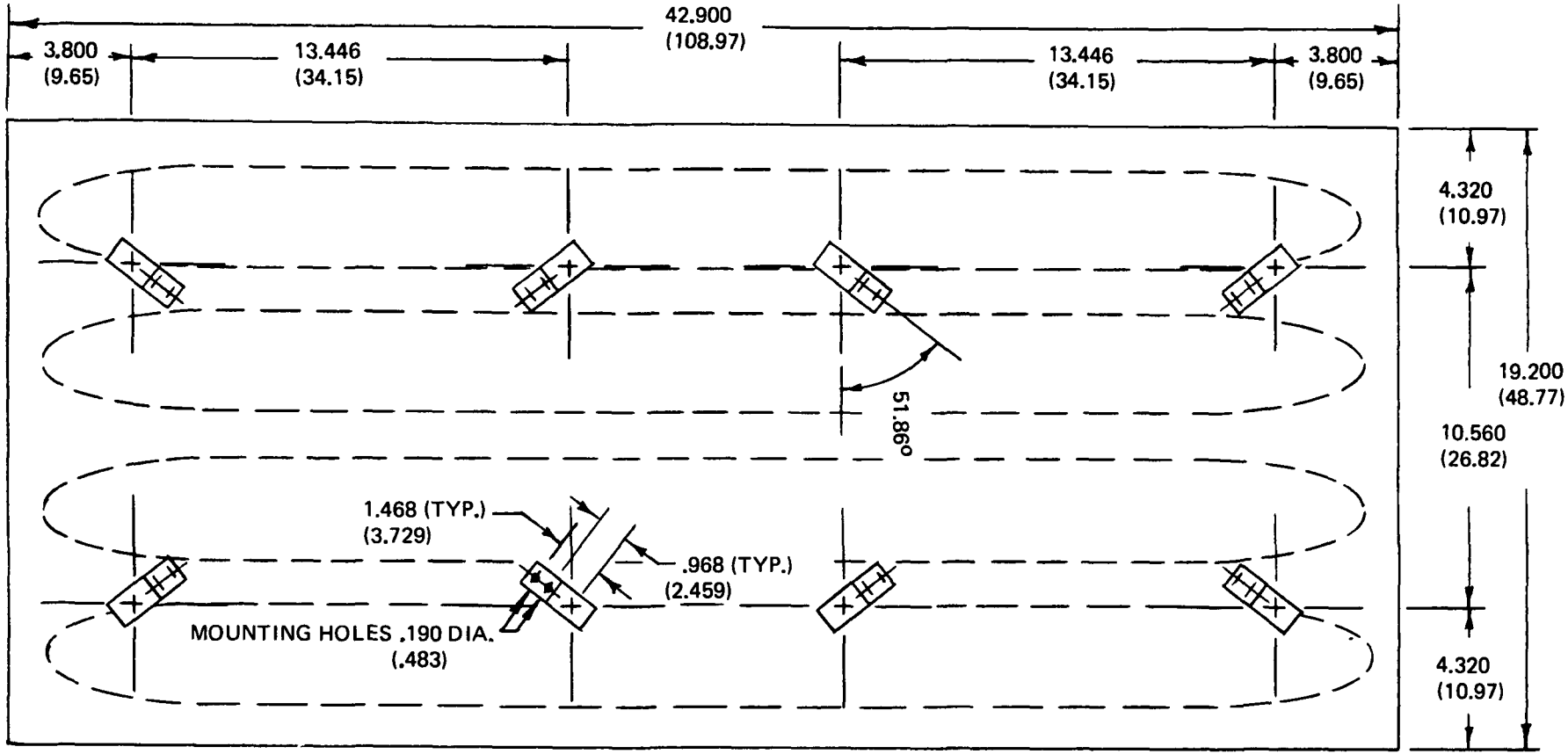

PANEL UPPER SURFACE VIEW

DIMENSIONS: INCHES
(cm)

Figure 7. HEAT SHIELD STANDOFF CLIP INSTALLATION

PANEL FABRICATION

The methods used to manufacture the René 41 panels are an extension of the technology developed for manufacturing aluminum panels during the initial phase of the advanced structural panel program. This technology features an incremental brake-forming approach which has been shown to be cost effective compared with conventional methods of forming trapped beads. The brake-forming approach also permits greater versatility in selecting bead cross section geometry, and it eliminates thinning of the material at the crown of the bead caused by stretching in the conventional forming methods. Both of these features are necessary to design and produce minimum weight beaded and tubular structural panels. The rationale for, and the development of, the incremental brake-forming method are discussed in more detail in reference 9.

The principal difference between manufacturing the aluminum panels and the René 41 panels is the assembly method. The aluminum panels, which were tested at room temperature, were assembled by bonding with the end closure region reinforced with rivets. Considerations of fabrication cost, mass efficiency, and high temperature aging and test environments resulted in the selection of welding for assembly of the René 41 panels.

The manufacturing sequence for producing the René 41 advanced structural panels is outlined in figure 8. The various stages indicated are discussed in more detail in the following subsections.

Uniform Section Forming

The uniform section forming technique consists of forming each bead separately in a mechanical press brake. A two part die is used to wrap the bead around a male mandrel. The dimensions of the mandrel include springback factors, so that the bead will have the desired radius and bend angle after release from the tool. This method eliminates thinning of the material which is inherent in conventional methods of forming trapped beads.

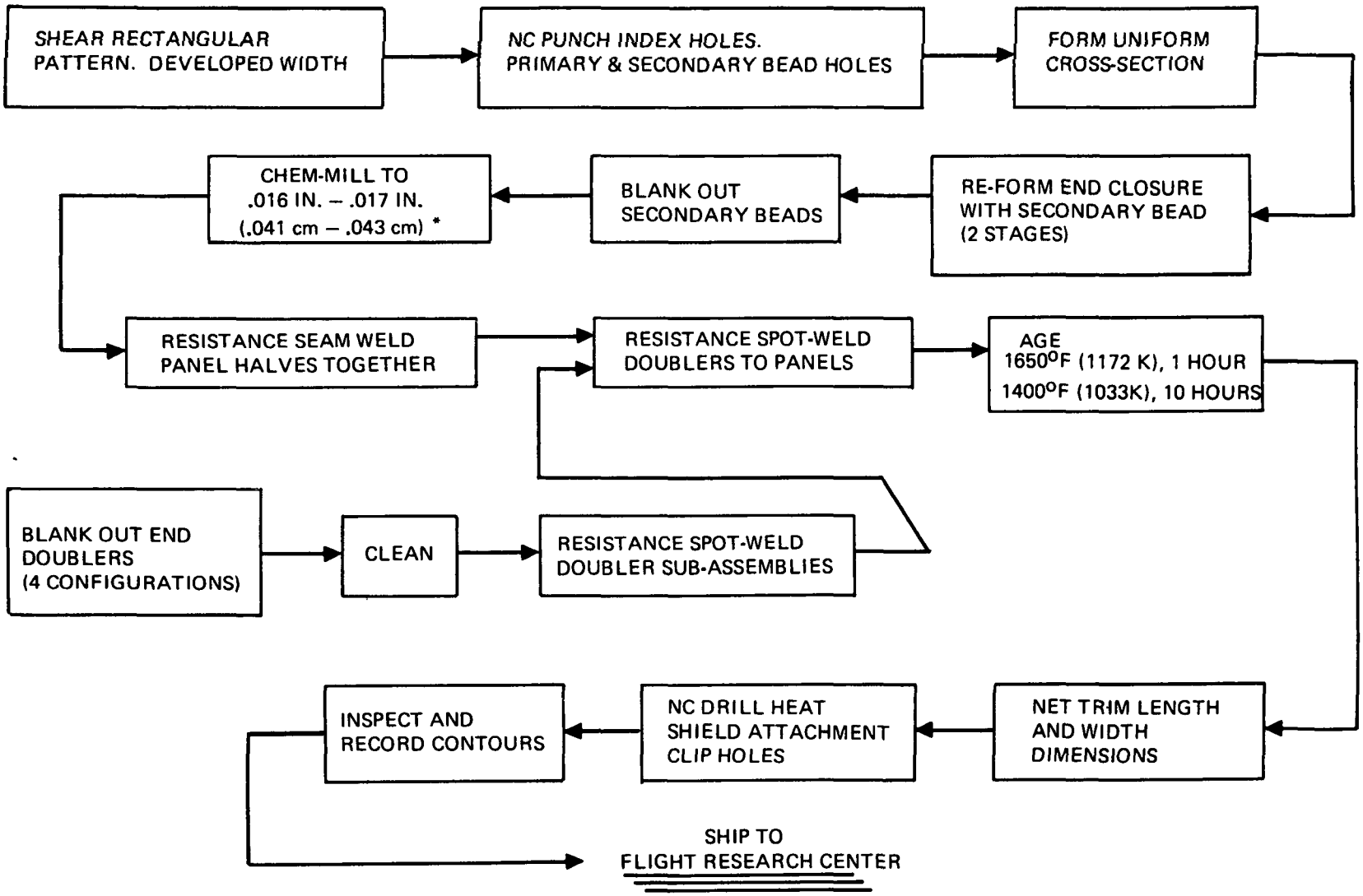

* AS-RECEIVED MATERIAL THICKNESS = 0.0185 INCH (.047 cm)
MINIMUM GAUGE RESTRAINT = 0.0160 INCH (.041 cm)

Figure 8: MANUFACTURING SEQUENCE FOR PRODUCING RENE' 41 ADVANCED STRUCTURAL PANELS

The forming sequence for the configuration 2 cross section is illustrated in figures 9 through 12. Each bead element is formed individually by wrapping the bead and setting the 2t bend radii at the bead-flat intersections at the end of the forming stroke. In figure 9 the flat blank of 0.018 in (0.046 cm) René 41 stock is shown being positioned in the tool prior to the forming stroke. Sheared dimensions of the flat blank were 22.3 x 44.3 inches (56.6 x 112.5 cm) for a nominal excess in developed width of 0.5 in. (1.3 cm), and in overall length of 1.4 in. (3.6 cm). Index holes were punched by numerical control at 2.593 in. (6.586 cm) intervals in surplus material at the ends of the blank to locate the centerline of each primary and secondary bead. Figure 10 shows an end view of the forming tool with the blank in place. One bead has already been formed and the forming stroke is beginning to wrap the second bead. Figure 11 shows the completion of the forming stroke which sets the 2t bend radii at the bead-flat intersections. The 2t bend radius of the female die has been increased to approximately 10t at the ends of the tool so that the bead-flat mold line will not interfere with reforming of the end closures. In figure 12 the press is opening and the formed bead is released showing springback of the material from the tool contour.

In figure 13 two sheets are shown with the uniform section forming completed. These two sheets will eventually constitute two halves of a tubular panel subassembly.

The forming sequence for the configuration 2A cross section is similar to that just described, except that two stages are required as follows:

> First stage--wrap flute and side radii of basic bead element in a continuous sine-wave type configuration, and form the 2t bend radii at the bead-flat intersection.
>
> Second stage--set the 2t bend radii and angle at the flute-sidewall intersection.

A more detailed description of this two stage forming sequence for fluted beads can be found in reference 9.

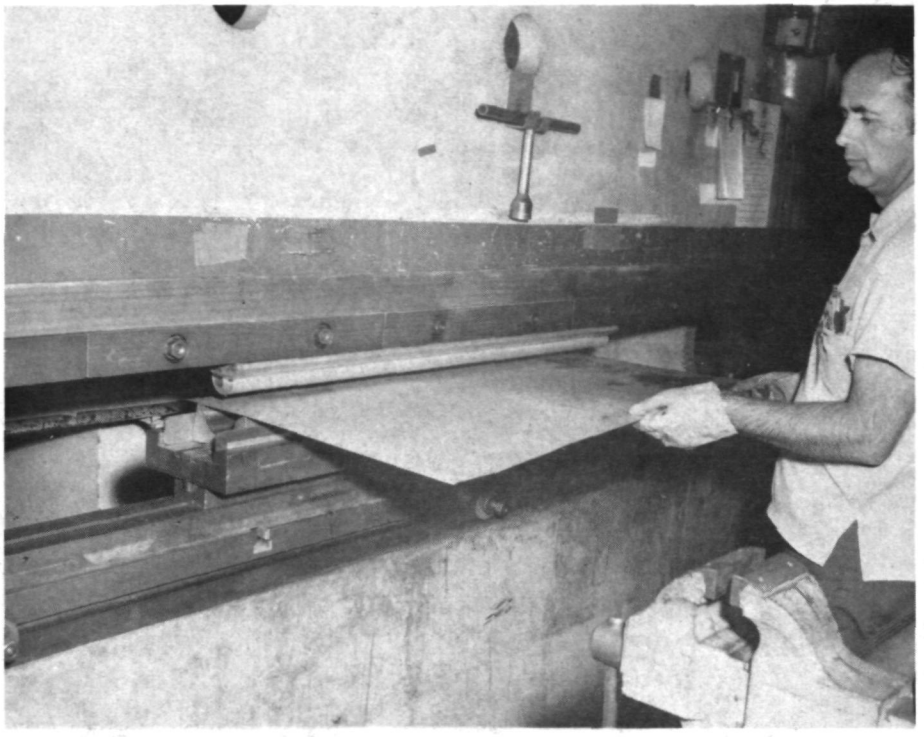

Figure 9: FLAT BLANK POSITIONED IN UNIFORM SECTION FORMING TOOL

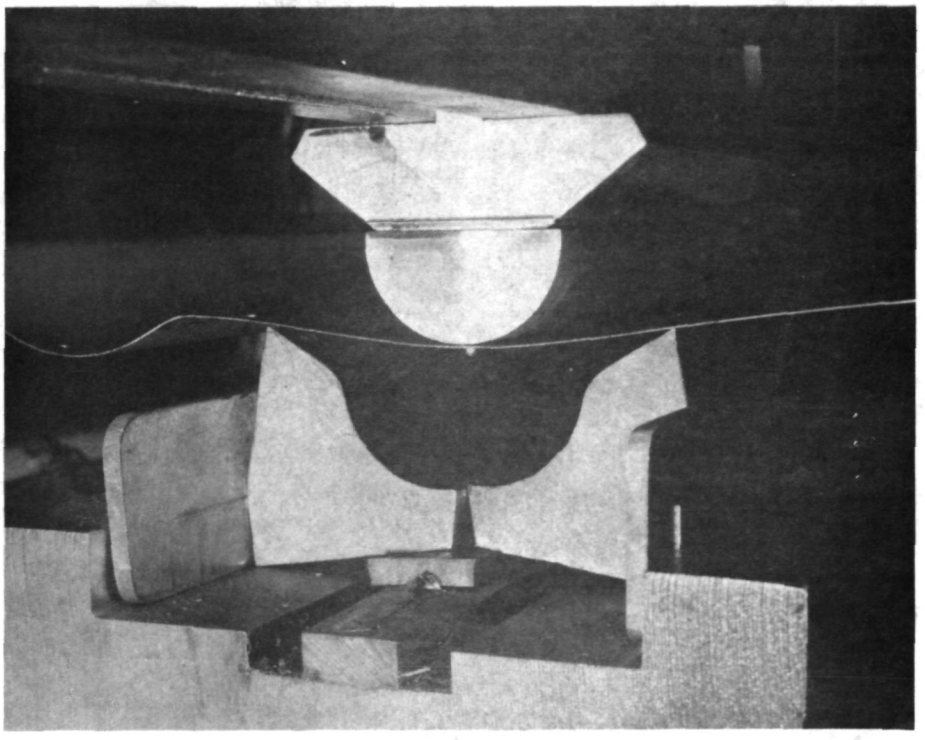

Figure 10: UNIFORM SECTION FORMING–BEGINNING OF STROKE

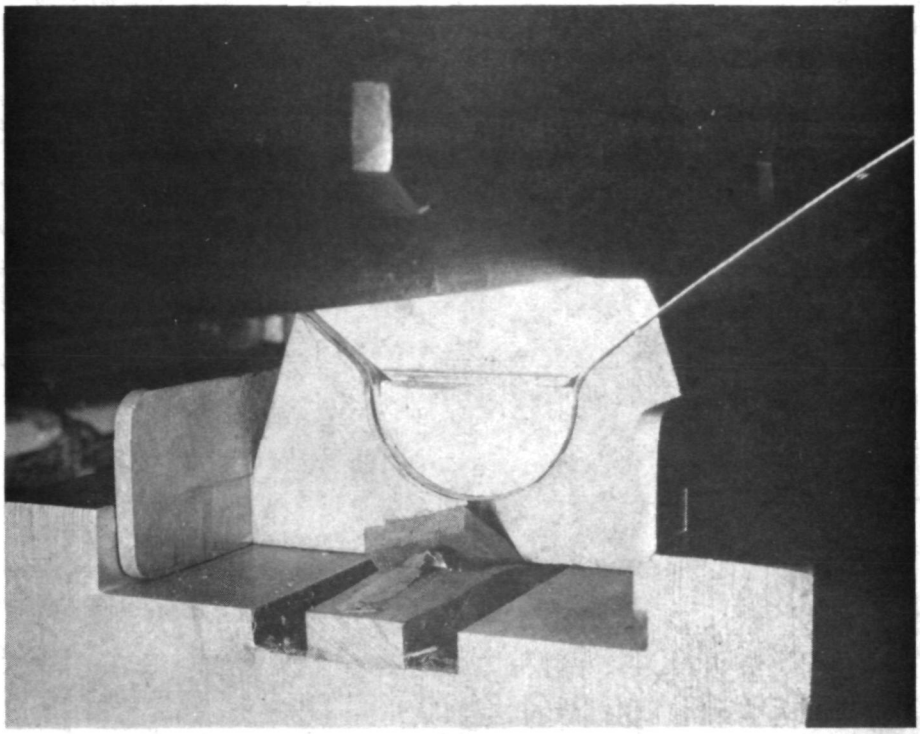

Figure 11: UNIFORM SECTION FORMING–COMPLETION OF STROKE

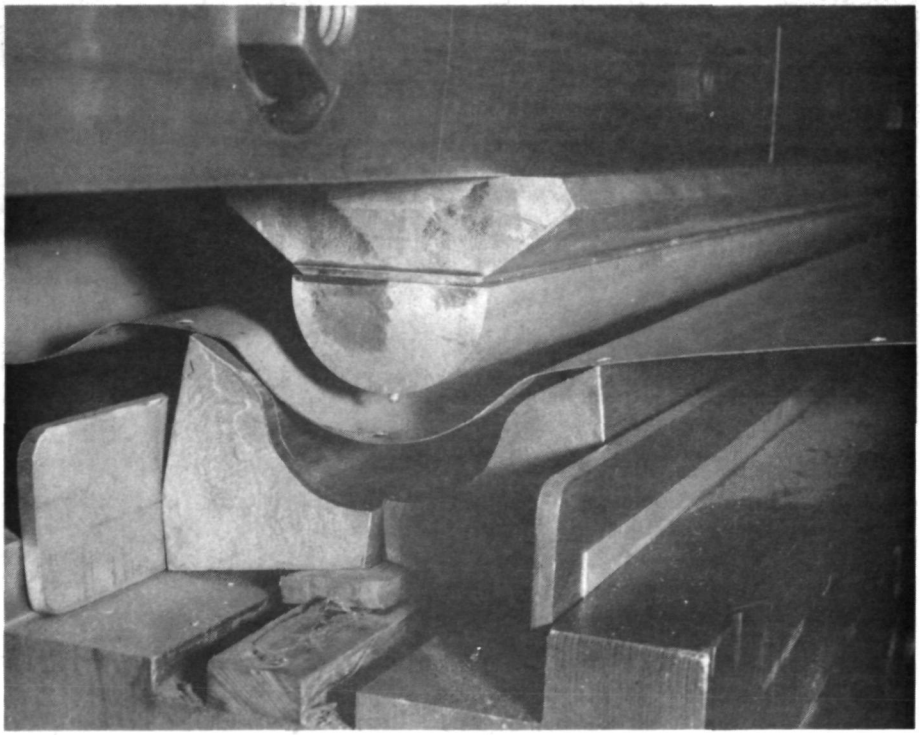

Figure 12: UNIFORM SECTION FORMING–PART RELEASED SHOWING SPRINGBACK FROM TOOL CONTOUR

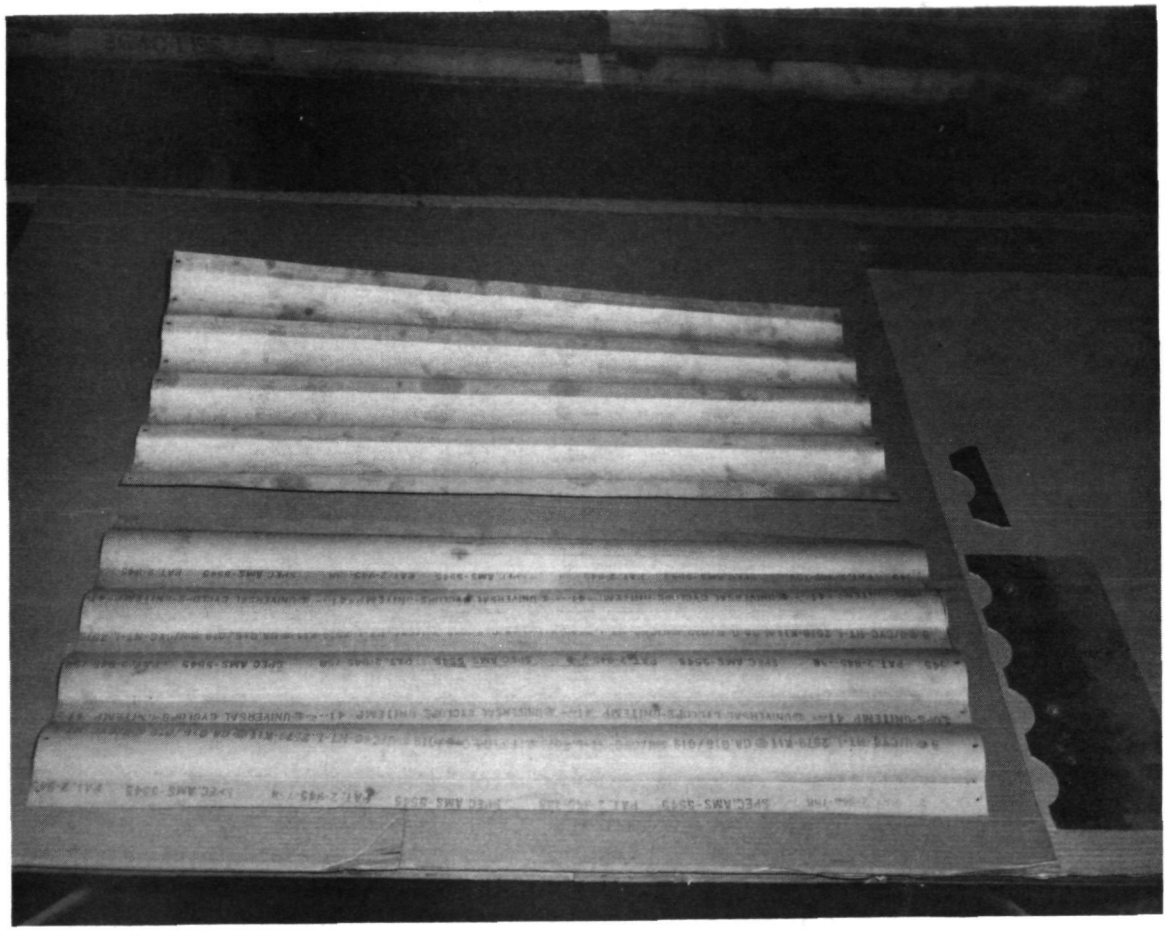

Figure 13: PANEL HALVES WITH UNIFORM SECTION FORMED

End Closure Forming

The panel end closures are produced by reforming the ends of the uniform section bead. This is basically a shearing type of deformation in which compression buckling is minimized by forming secondary beads in the flats between the primary bead end closures. The secondary beads pull the excess material away from the primary bead end closures during forming. When forming is complete the secondary beads take up the difference between the net panel width and the developed width of the uniform section.

The René panel end closures were formed in two stages, which also helped to control compression wrinkling. The first stage formed the basic flat area and the secondary bead, allowing partial free forming of the primary bead closure. The second forming stage sized the primary bead closure and slightly raised the height of the secondary bead. Spring loaded clamp plates were used in both stages to prevent severe wrinkle formation.

The first stage forming tool is shown in figure 14. The female die is in the foreground, the male part with clamping springs is in the background, and the clamping plate lies between them. The second stage forming tool is shown similarly in figure 15. Figure 16 shows the workpiece, with the formed uniform section, positioned in the tool ready for first stage end closure forming. The same workpiece is shown in figure 17 after completion of the first stage forming stroke. The secondary bead with its locating pin and the partially formed primary bead closure are clearly seen.

The workpiece with end closure forming completed is shown in figure 18. Some compression wrinkling is evident in the flats. Hand planishing was applied in these areas to improve flatness prior to assembly. Also prior to assembly, the secondary beads were removed (see discussion under PANEL DESIGN - Panel End Closure) by a simple blanking operation. Shims cut with the same blanking die were installed during final assembly to fill the spaces vacated by blanking out the secondary beads.

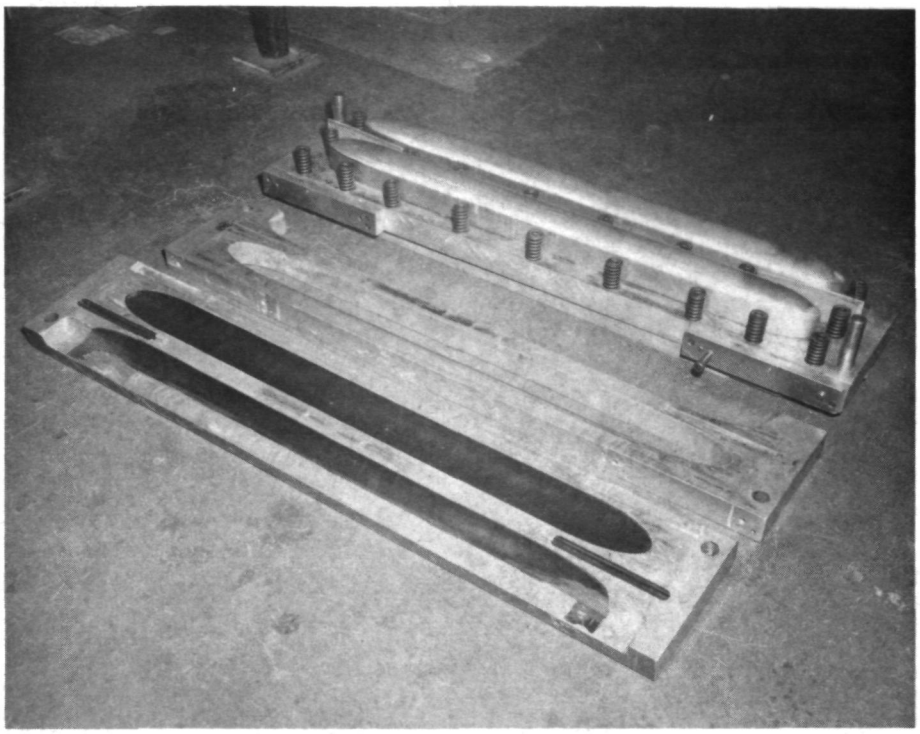

Figure 14: FIRST STAGE END CLOSURE FORMING TOOL

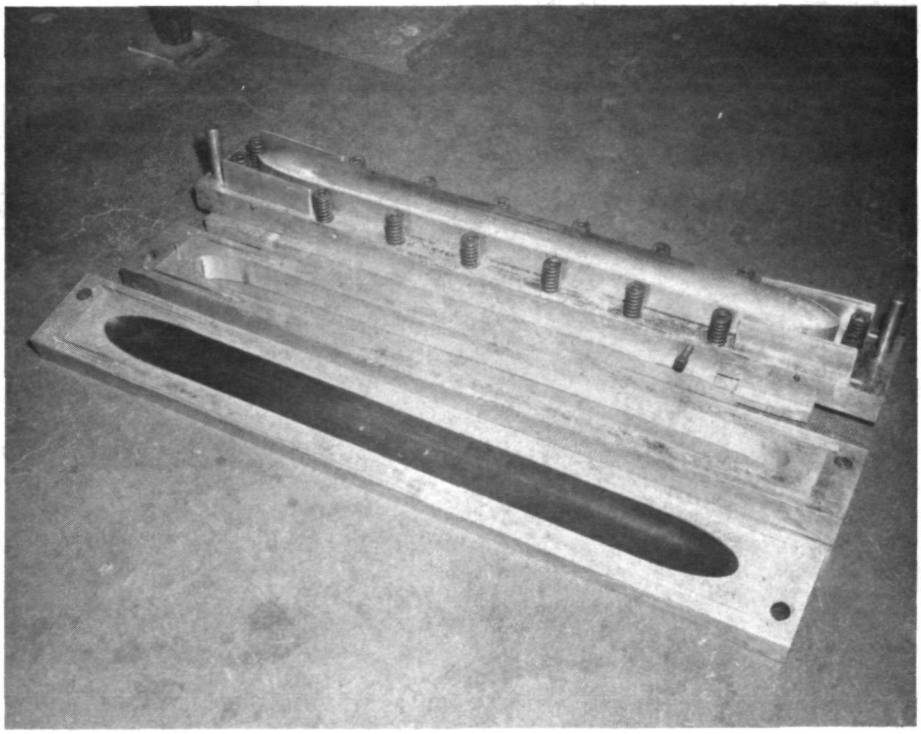

Figure 15: SECOND STAGE END CLOSURE FORMING TOOL

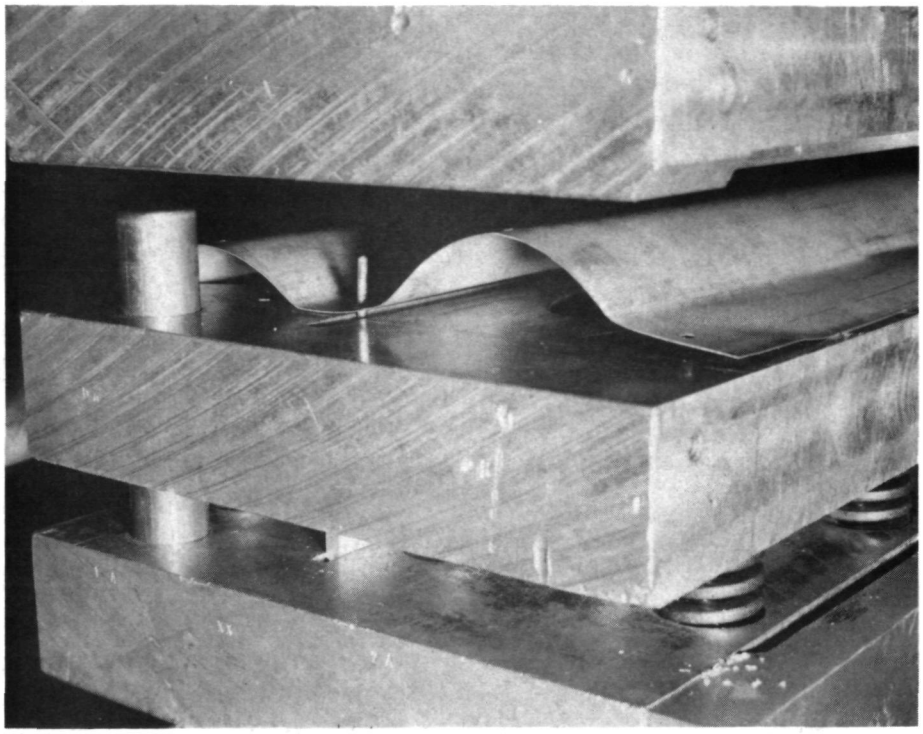

Figure 16: PANEL UNIFORM SECTION POSITIONED FOR FIRST STAGE END CLOSURE FORMING

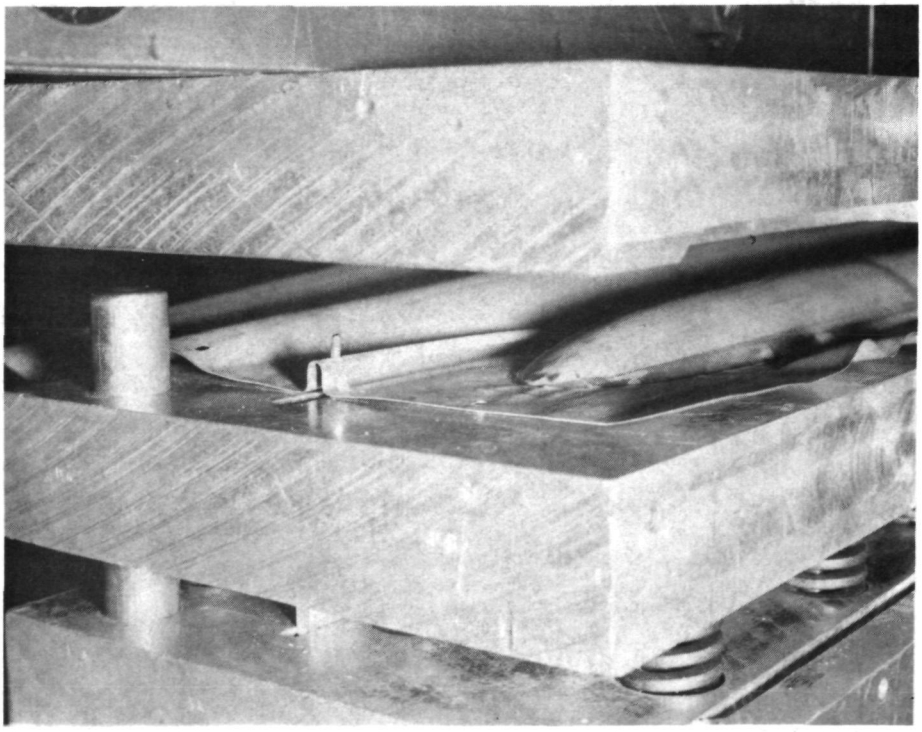

Figure 17: END CLOSURE AFTER COMPLETION OF FIRST STAGE FORMING STROKE SHOWING SECONDARY BEAD

Figure 18: PANEL HALF WITH UNIFORM SECTION AND END CLOSURES FORMED

Further study of the end closure forming operation appears to be warranted for production applications. Variations in both the configuration and the forming sequence should be investigated to arrive at an end closure that can be produced without any compression wrinkling.

Doublers

Doublers consisted of two layers per side of 0.018 in. (0.046 cm) thick material, contoured as shown in figures 4 and 5. These were fabricated by shearing to overall width and length dimensions, punching index holes, blanking out the bead outline with a nominal 0.05 in. (0.13 cm) clearance, and hand trimming the tapered finger portions. The blanking operation is seen in figure 19.

The doubler pairs were spot welded into subassemblies prior to final panel assembly. For production applications it is recommended that doublers be fabricated from one thickness of material, 0.036 in. (0.091 cm), and chem-milling to obtain reduced thickness transitions. This would eliminate the operation of welding doubler pairs into subassemblies and would facilitate spot welding of the final panel assemblies.

Assembly

Four assembly methods were considered for the René 41 advanced structural panels:

1) riveting
2) brazing
3) fusion welding
4) resistance welding

Riveting was excluded because of the weight penalty and the difficulty of drilling and deburring small holes in the René 41 alloy which would result in high manufacturing costs. Brazing was excluded because of anticipated high costs for process development and tooling and because of complications in the heat treat cycle.

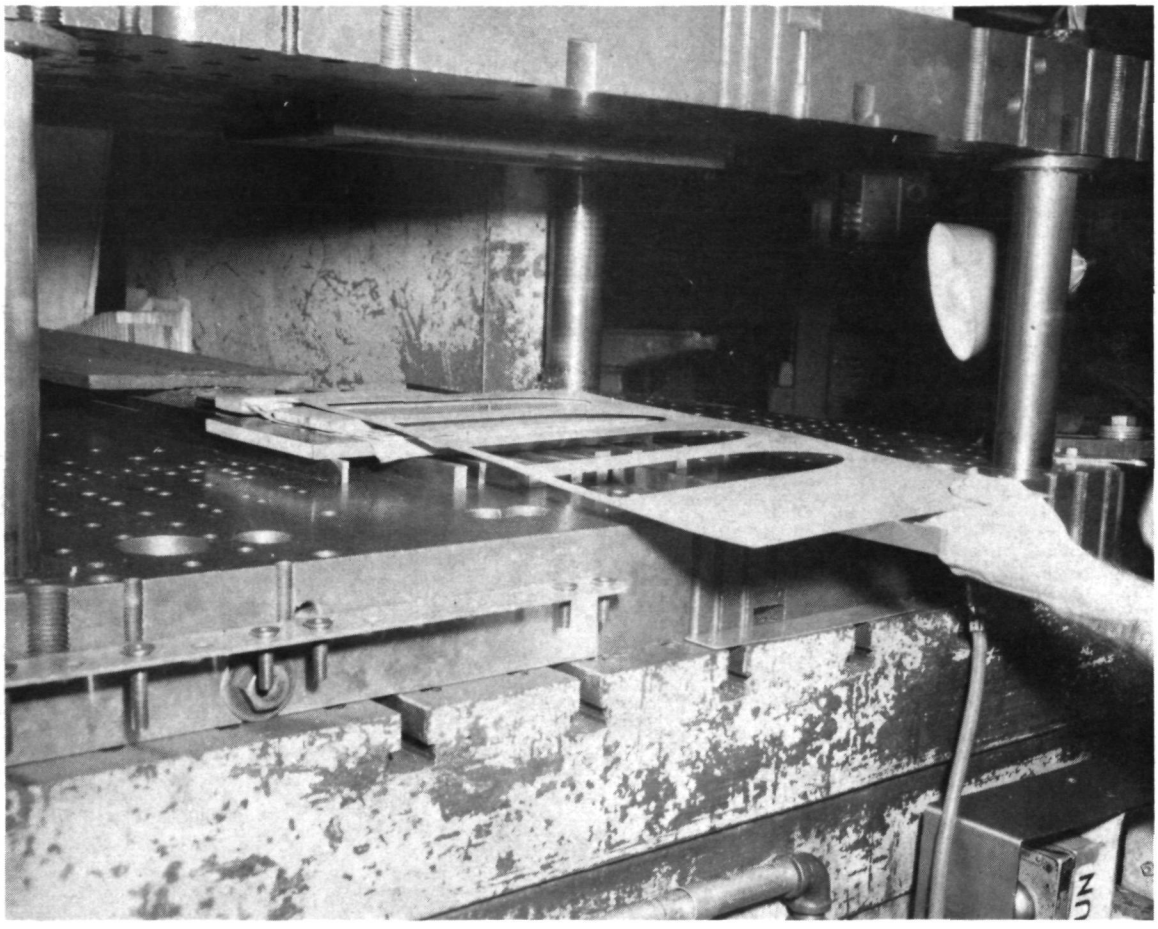

Figure 19: BLANKING OF DOUBLER CUTOUTS

Comparative tests were conducted between fusion welding (electron beam) and resistance welding (roller seam and spot). Resistance welding was selected initially because of its economy and versatility. However, electron beam welding was investigated as the only practical method of attaching tapered thickness doublers to the panels with a continuous weld path. Electron beam welding was abandoned when compression buckling occurred in the bead sidewalls as a result of shrinkage in the adjacent weld seam. It was concluded that extensive development of restraint fixturing and additional thermal treatment would probably be required to overcome this problem. Instead of attempting to overcome the fusion welding problems, it was decided to taper the doubler fingers in planform rather than in thickness and to attach them by resistance welding.

Roller seam welding was used for joining the two panel halves. Figure 20 shows the panel halves clamped together in preparation for seam welding. Figure 21 shows the panel subassembly in the roller seam welding process. Figure 22 shows the finished panel subassembly. Three seam welds run lengthwise in the interior flats and two seams along each exterior flat. The seams adjacent to the beads are continued around the end closures and out to the panel edges. Additional short longitudinal seams are added to the end closure flat areas.

Figure 23 shows doubler pairs being spot welded together to form a doubler subassembly. Doubler and panel subassemblies are clamped together as shown in figure 24 in preparation for final assembly. At this stage the shims have been added to fill in the spaces vacated by blanking out the secondary beads.

Figure 25 shows the spot welding of the panel final assembly. The final spot welds to join the doubler and panel subassemblies were made through the original two sheet nuggets formed when spot welding each doubler pair. This procedure minimized interface tolerance problems by absorbing weld penetration variations in the thick doubler nugget rather than in the thin outer doubler ply.

Panel and end closure joining operations would be simplified by the use of thicker doubler material, chem-milled as necessary to obtain reduced thickness transition. Resistance welding of 4-sheet stackups of similar thickness plies remains a marginal process with current facilities and techniques. This problem can be resolved by using chem-milled doublers with increased thickness pads on outer plies for the spot weld nugget.

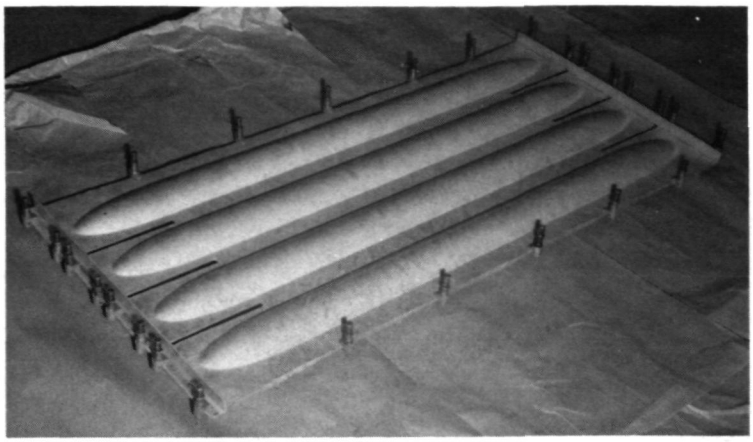

Figure 20: PANEL HALVES CLAMPED TOGETHER PRIOR TO SEAM WELDING

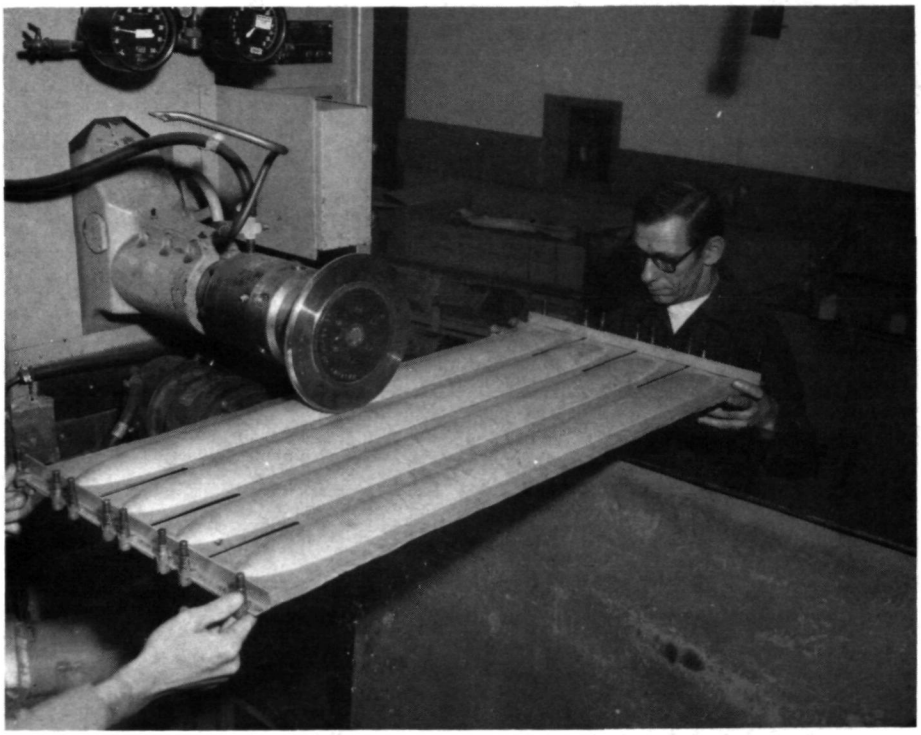

Figure 21: SEAM WELDING OF PANEL SUBASSEMBLY

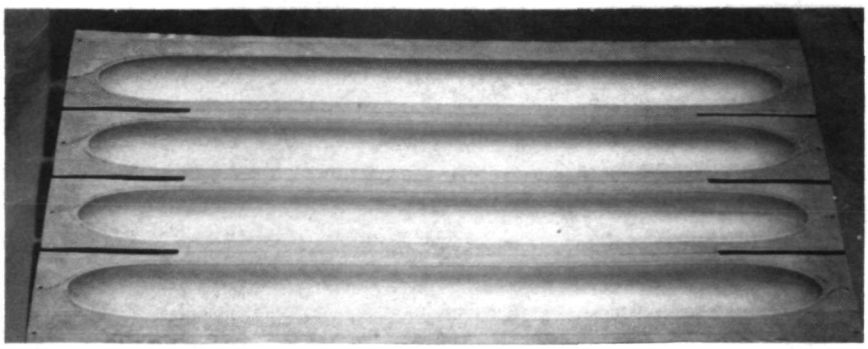

Figure 22: PANEL SUBASSEMBLY WITH SEAM WELDING COMPLETED

Figure 23: SPOT WELDING DOUBLER SUBASSEMBLY

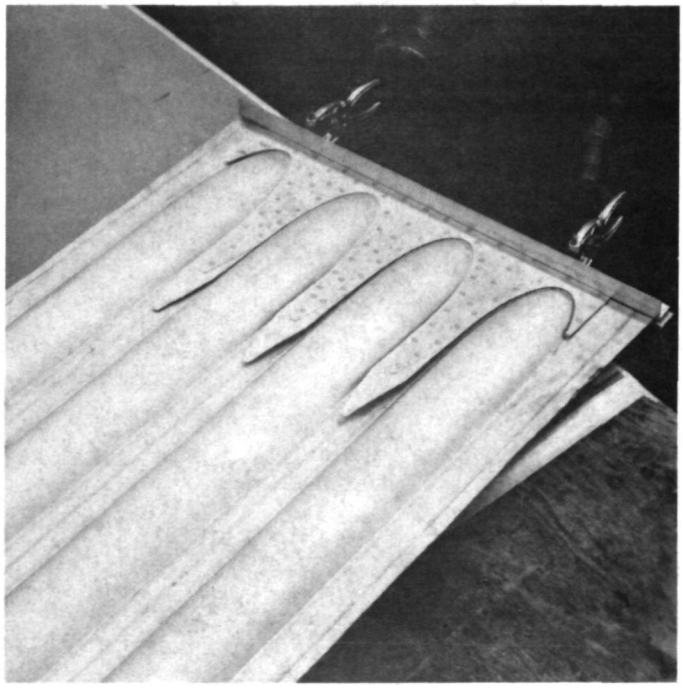

Figure 24: DOUBLER AND PANEL SUBASSEMBLIES CLAMPED PRIOR TO FINAL ASSEMBLY

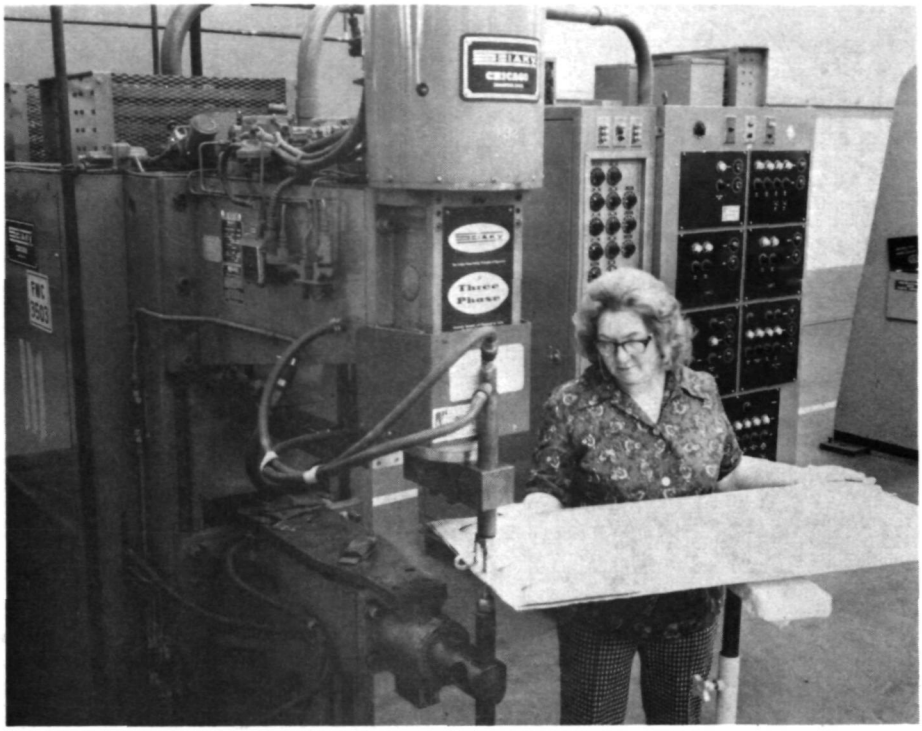

Figure 25: SPOT WELDING PANEL FINAL ASSEMBLY

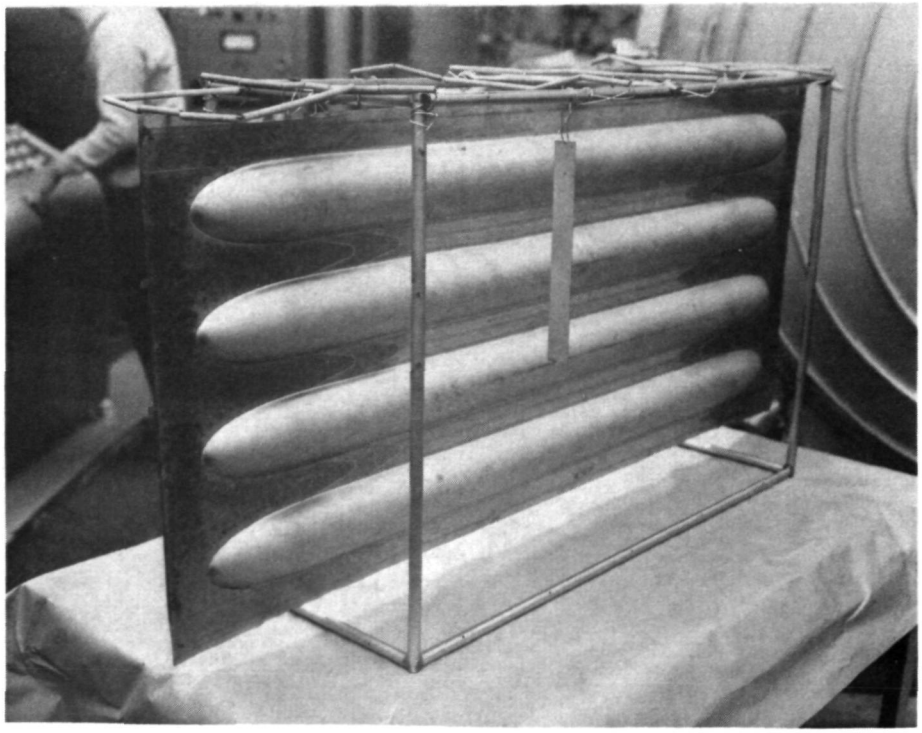

Figure 26: PANEL FINAL ASSEMBLY MOUNTED IN AGING RACK

Heat Treatment

Heat treatment applied to the René 41 panels consisted of a dual age after final weld assembly. Material was procured in the solution annealed condition, 1975°F (1352 K). After welding but prior to net trim operations, the panels were aged at 1650°F (1172 K) for one hour, followed by 1400°F (1033 K) for ten hours. This cycle was established from previous experience with René 41 to minimize strain-age cracking tendencies without large sacrifices in tensile strength. Aging was accomplished in a cold wall, radiantly heated vacuum furnace to prevent surface embrittling from oxidation at the 1650°F (1172 K) temperature. As a precaution against outgassing problems, vent holes were drilled in the beads at one end on the bottom side of the panel and in the flats between seam welds near the panel center, and the temperature was held for 15 minutes at 600°F (589 K) and 800°F (700 K) during heat up. No formal fixturing was required; panel assemblies were suspended from a simple rack as shown in figure 26. Figure 27 shows the vacuum furnace with a panel assembly ready to be installed for aging.

Panel Specimens

Six panels of the configuration 2 design were fabricated and delivered to the NASA Flight Research Center for future testing at elevated temperature in the hypersonic wing test structure.

After assembly and heat treating the panels were trimmed to final size in a conventional horizontal milling machine set up with an abrasive cutoff wheel using freon lubricant. Mounting holes for heat shield standoff clips were drilled on a tape controlled NC drill press. Net panel dimensions and clip mounting hole locations are seen in figure 7. Figure 28 shows one of the finished panels ready for packaging and shipping.

Panel cross section geometry was checked on three of the panels selected at random. Plastic molds were cast covering the entire width on one side of each panel at three locations: at the transverse centerline, and approximately ten inches on either side of the transverse centerline. These molds

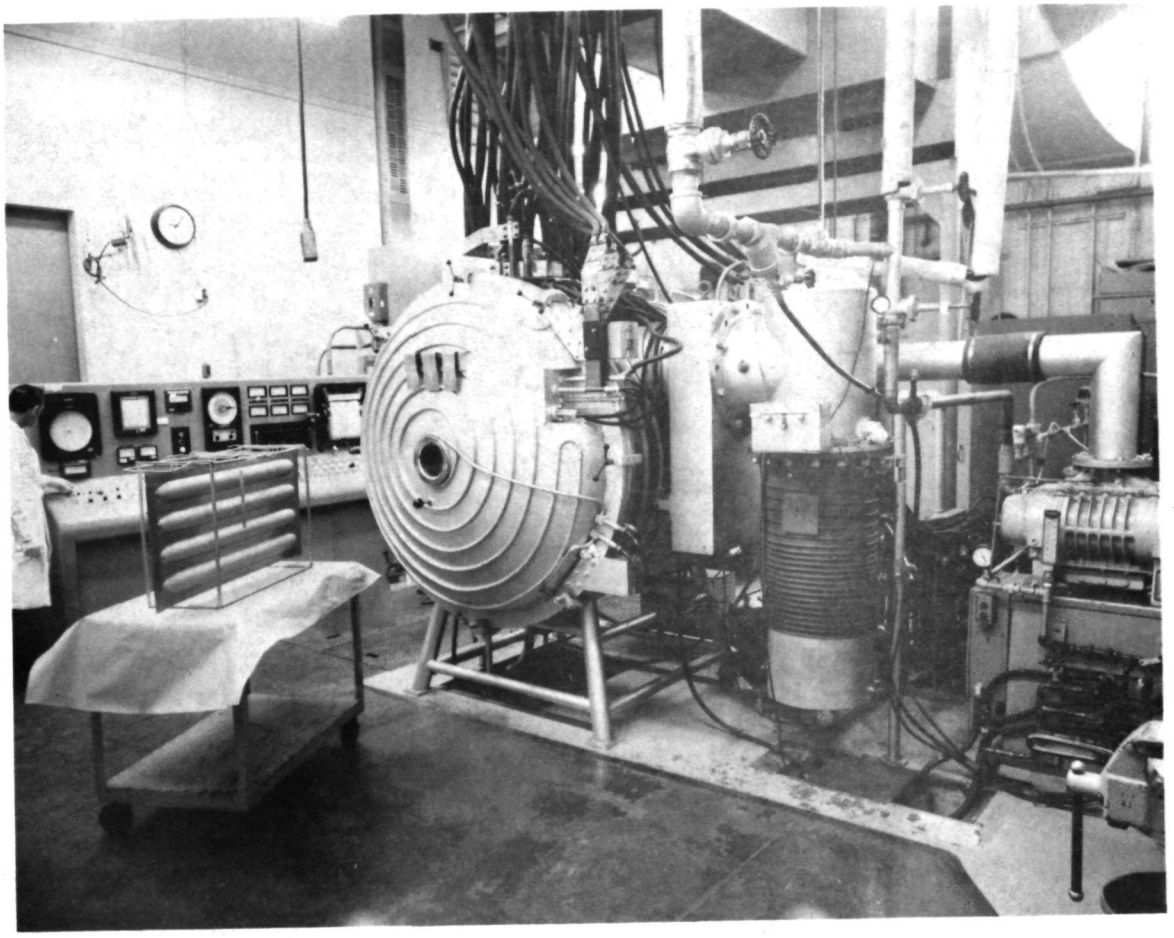

Figure 27: VACUUM FURNACE WITH PANEL FINAL ASSEMBLY READY FOR AGING

provided profiles of the uniform cross section geometry which were carefully traced and measured. Average values of the fabricated cross section dimensions so determined are compared with nominal design values below:

		BEAD RADIUS	BEAD HEIGHT	BEAD WIDTH	FLAT WIDTH
DESIGN VALUE	in.	1.781	0.8905	3.085	1.452
	(cm)	(4.524)	(2.262)	(7.836)	(3.688)
MEASURED VALUE	in.	1.701	0.8955	3.066	1.472
	(cm)	(4.321)	(2.275)	(7.788)	(3.739)
DIFFERENCE	%	-4.5%	+0.6%	-0.6%	+1.4%

Except for the bead radius, differences between measured and design values are minor. The bead radius measurements were taken over a 60° arc at the crown of the bead. The bead radii appeared to increase to values considerably larger than the design value adjacent to the flats. This variation in bead radius is due primarily to chem-milling of the sheets after forming which affected the springback characteristics of the remaining material. (Chem-milling was accomplished after forming because forming tools were developed for material with a thickness of 0.018 - 0.0185 inch (0.046 - 0.047 cm) prior to a decision to chem-mill the sheets to bring them closer to the design thickness of 0.016 inch (.041 cm).) For production applications prior negotation with the supplying mill could achieve closer material thickness control, thus eliminating the chem-milling step and resulting in better overall configuration control.

Thicknesses of the formed and chem-milled sheets were measured randomly in several places prior to assembling the panels. Thickness values ranged from 0.0165 in. (0.042 cm) to 0.017 in. (0.043 cm). Further thickness reduction was not attempted because of the risk of seriously reduced local buckling strengths if the final thickness were less than the design value of 0.016 in. (0.041 cm) at any place near the crown of the bead.

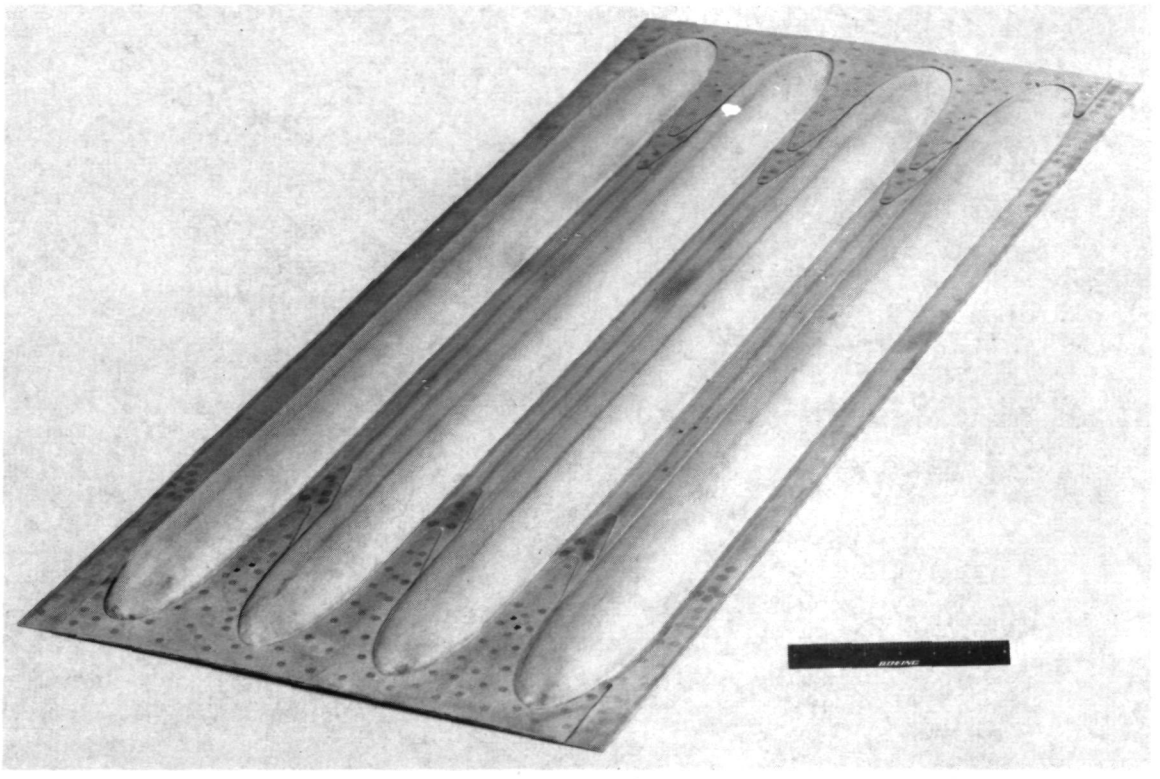

Figure 28: RENE' 41 ADVANCED STRUCTURAL PANEL

Panel components were weighed prior to assembly, and the finished mass of one panel was obtained after net trim but before drilling. Masses are summarized below:

	Pounds	(kg)
Mass of formed panel half with shims (untrimmed)	5.05	(2.290)
Doubler parts, one end of panel (untrimmed)		
bottom, short	0.364	(0.165)
bottom, long	0.415	(0.188)
top, short	0.463	(0.210)
top, long	0.553	(0.251)
Panel subassembly (untrimmed)	10.10	(4.581)
Doubler subassemblies (untrimmed)	3.59	(1.628)
Panel assembly (untrimmed)	13.69	(6.210)
Panel assembly (trimmed)	12.80	(5.806)

Finished masses of panel components were not available because they were not trimmed to final size until after the panels were assembled. However, their approximate mass can be inferred by comparing the mass of the panel assembly before and after trimming. By this reasoning the mass of the uniform section of the fabricated panel is determined to be 1.651 lbm/ft^2 (8.106 kg/m^2). Comparing this value to the design mass of 1.569 lbm/ft^2 (7.668 kg/m^2) indicates that the average sheet thickness is 0.0168 in. (0.0426 cm), which is 5 percent greater than the nominal design value of 0.016 in. (0.041 cm).

The joint mass penalty is 36%, which is twice that found for similar aluminum panels in reference 8. The higher joint weight penalty for the René 41 panels can be attributed to excess doubler weight. Doublers were made thicker

than necessary for strength in order to be compatible with the existing hypersonic test structure and beaded panels. By optimizing the design of the end closures and doublers specifically for the tubular panels, the joint weight penalty could be reduced considerably.

End Closure/Local Buckling Specimens

Small size, end closure/local buckling specimens were fabricated and tested prior to fabricating the panel specimens. Three specimens of each design were fabricated and tested to demonstrate adequate strength in the end closures and to verify the local buckling analysis equations used in designing the panels. The results of these tests are discussed in the following section of this report, entitled TESTING.

The same tooling developed for the panel specimens was used in forming the end closure/local buckling specimens, and essentially identical processing was applied in assembly and heat treating.

These specimens were narrower than the panel specimens, having only three tubes instead of four. They were also shorter, with end closures formed at one end only. The open ends of the specimens were potted in tooling plastic for gripping and loading in the test fixture. Edge chords of aluminum T section were attached along the sides to stabilize the edges and to distribute shear loads into the specimen. Loads were applied to the specimens through the potting at one end and through aluminum angles attached back to back to form loading flanges at the other end. The edge chords and the loading flanges were attached to the specimen with number 10 size fasteners spaced at 1.75 in. (4.45 cm). Specimens to be tested in shear, and in combined compresssion and shear, were drilled at both ends for installation in the combined load local buckling test fixture described in reference 10. The ends of specimens to be tested in compression only were machined flat and parallel for loading in a universal test machine.

Typical end closure/local buckling specimens of the two configurations are shown in figures 29 and 30. The length of the specimens is 24 inches (61 cm), comprising 11 inches (28 cm) of end closure, including the doubler fingers, 9 inches (23 cm) of uniform section, and 4 inches (10 cm) of potting. The specimens shown have not been drilled for installation in the combined load local buckling test fixture. The short channel sections on either side of the specimens at the potted ends help achieve uniform load distribution by transmitting applied compression loads into the edge chords.

The end closures of the fluted tubular specimens differed slightly from the original design. Instead of extending the flutes out to the extreme end of the bead closure, as indicated in figure 3, they were continued parallel from the uniform section until they intersected the surface of the bead closeout. Thus, the flutes end about 2.1 inch (5.3 cm) short of the end of the bead closeout, as seen in figure 30. This modification of the original design was expected to give adequate end closure strength while reducing the cost of tool development.

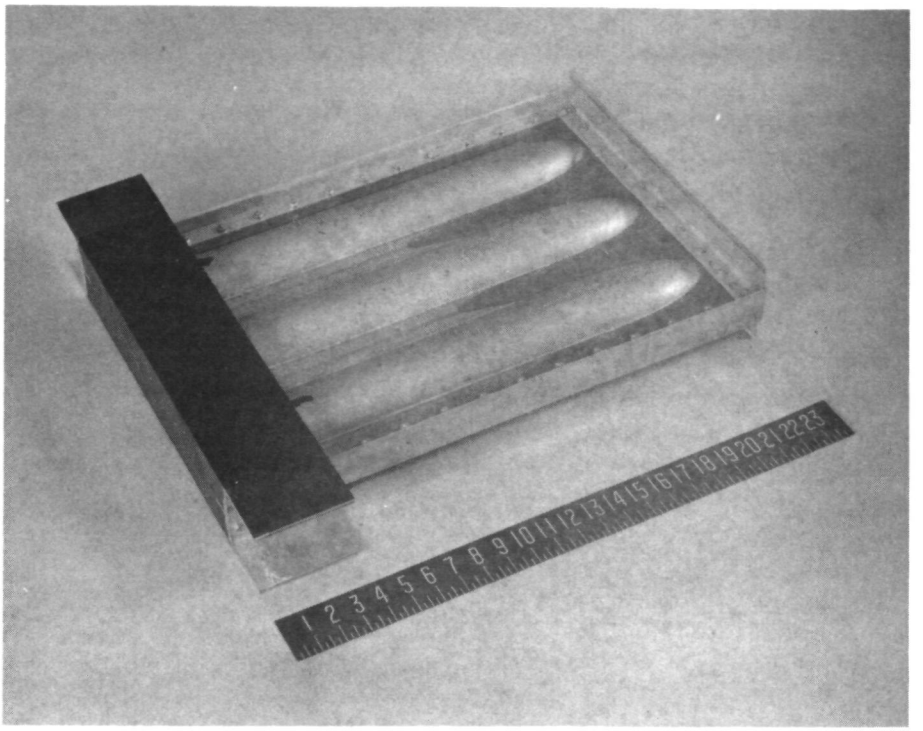

Figure 29: END CLOSURE/LOCAL BUCKLING TEST SPECIMEN– CONFIGURATION 2

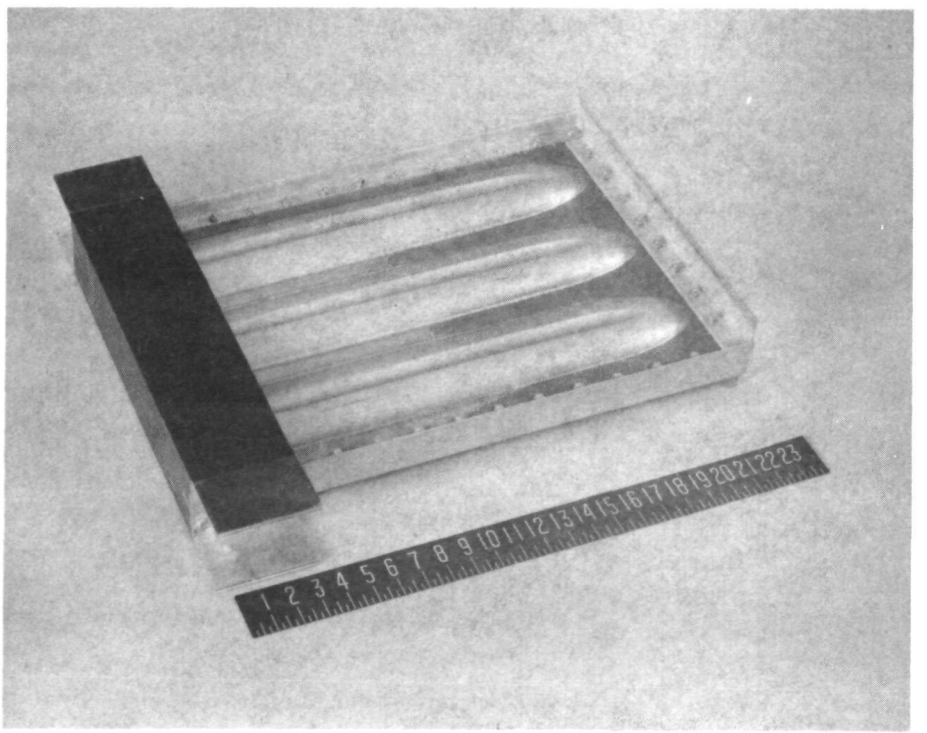

Figure 30: END CLOSURE/LOCAL BUCKLING TEST SPECIMEN– CONFIGURATION 2A

TESTING

Six 43 in. x 19 in. (109 cm x 48 cm) René 41 panels were fabricated as described in the preceding section of this report, and delivered to NASA Flight Research Center where they will be tested under combined loads of compression and shear at elevated temperature. In support of this work, end closure/local buckling specimens were tested at room temperature for the dual purpose of demonstrating adequate end closure strength to transmit design and test loads into the panel specimens, and to verify the local buckling equations used in the panel design and analysis. Three end closure/local buckling specimens for each of the two panel configurations were fabricated and tested. For each configuration, one specimen was tested in compression, one in shear, and one in combined compression and shear. Typical specimens of the two configurations are seen in figures 29 and 30.

The compression only specimens were tested in a 300 kip (1335 kN) universal test machine. Eight strain gages were installed on the uniform section of each specimen in the longitudinal direction to control uniformity of load application and to monitor maximum compressive strains in the tube walls. The shear and the combined compression and shear specimens were tested in the combined load local buckling test fixture which was designed and used earlier for testing similar beaded and tubular aluminum local buckling and end closure specimens. A description of this test fixture is contained in reference 10. Each shear test specimen was instrumented with four longitudinal strain gages and two strains rosettes in the uniform section to monitor load uniformity and maximum stresses in the tube walls. Each combined load specimen was instrumented with six longitudinal strain gages and two strain rosettes used similarly. All of the shear and combined load specimens were instrumented with moiré grid to monitor distortions in the end closure flat regions during loading.

All specimens were loaded incrementally. After each increment of load was applied, strain gage data were read and recorded manually, using a speedomax readout system, and photos of the moiré fringe patterns were taken. Load was increased until failure occurred.

Results of the end closure/local buckling specimen tests and analytically predicted failure loads for the panel specimens are presented and discussed in the following subsections.

End Closure/Local Buckling Test Results

Maximum test loads applied to each of the six end closure/local buckling specimens are given in figure 31 and are compared with predicted failure loads for the full size, 43 in. x 19 in. (109 cm x 48 cm) panels when loaded in the same condition. The first character group in the specimen identification number indicates the configuration: 2 is the circular arc tubular configuration; 2A is the fluted tubular configuration. The last character group indicates the test load condition: C for compression, S for shear, and CS for combined compression and shear. The test loads given do not necessarily represent maximum end closure strengths, since most failures were due to local buckling of the tube walls in the uniform section of the specimen. Therefore, the margins of safety indicated in the figure are lower bounds. They indicate adequate end closure strengths for both panel configurations to transmit full panel design loads and predicted maximum panel test loads over the range of proposed test load conditions.

Local buckling test failure stresses are compared with those predicted by the analysis in figure 32. The analysis consists of the local buckling equations described in reference 8. In the case of the circular arc tubular specimens, type 2, these equations include the modifications made to achieve correlation with the aluminum panel test results as described in reference 8. In the case of the fluted tubular specimens, type 2A, the original equations given in Section 12, "Static Strength Analysis," of reference 8 are used, since satisfactory correlation of analysis with tests of the fluted aluminum specimens was not achieved. The test results given in the figure are maximum stresses determined from strain gage readings at critical locations recorded during the tests. The poor correlation obtained with specimen 2A-R-E-2S is probably due to premature failure which initiated in the end closure at the flute runout. Failures of all other specimens appeared to be due to local buckling of the tube walls in the uniform section.

SPECIMEN NO.	MAXIMUM TEST LOADS LB/IN (kN/m)		MAXIMUM PREDICTED LOADS FOR FULL SIZE PANELS LB/IN (kN/m)		MARGIN OF SAFETY
	COMPRESSION	SHEAR	COMPRESSION	SHEAR	
2-R-E-1-C	2460 (431)	——	1225 (215)	——	1.01
2-R-E-2-S	——	930 (163)	——	618 (108)	.50
2-R-E-3-CS	1660 (291)	455 (79.7)	1079 (189)	296 (51.9)	.54
2A-R-E-1-C	2650 (464)	——	1079 (189)	——	1.46
2A-R-E-2-S	——	* 980 (172)	——	558 (97.8)	.76
2A-R-E-3-CS	1900 (333)	565 (99.0)	922 (162)	262 (45.9)	1.06

* END CLOSURE FAILURE, ALL OTHERS LOCAL BUCKLING FAILURES

Figure 31 END CLOSURE TEST RESULTS DEMONSTRATING ADEQUATE END CLOSURE STRENGTHS

SPECIMEN NO.	LOCAL BUCKLING STRESS - KSI (MN/m^2)		CORRELATION FACTOR (TEST/ANALYSIS)
	TEST	ANALYSIS (REF. 8)	
2-R-E-1-C	F_c = 67.4 (465)	F_c = 78.5 (541)	0.86
2-R-E-2-S	F_s = 36.8 (254)	F_s = 24.6 (170)	1.49
2-R-E-3-CS	F_c = 56.6 (390) F_s = 18.8 (130)	F_c = 46.9 (323) F_s = 15.6 (108)	1.21
2A-R-E-1-C	F_c = 75.4 (520)	F_c = 92.7 (639)	0.81
2A-R-E-2-S	F_s = 25.1 (173)*	F_s = 47.5 (327)	0.53
2A-R-E-3-CS	F_c = 79.3 (547) F_s = 21.3 (147)	F_c = 78.5 (541) F_s = 21.1 (145)	1.01

* END CLOSURE FAILURE

Figure 32 LOCAL BUCKLING TEST RESULTS AND CORRELATION WITH ANALYSIS

The correlation factors (correlation factor = test value/analytically predicted value) for the type 2 specimens indicate that the analysis which was verified by tests of aluminum panels is not adequate for the present René panel specimens. Several factors may have contributed to this poorer correlation:

1) The aluminum test data was obtained from specimens with deep beads (half angle approaching 90°), while the René test data presented here was obtained from specimens having much shallower beads (half angle equal to 60°, see figure 1). This difference in configuration may have had some effect on the correlation; however, the principal effect was probably caused by differences in the shape of the panel cross section from the design as shown in Figure 1.

2) Measured dimensions taken from the panel specimens are assumed to be representative of the end closure/local buckling specimens since both types of specimens were formed using the same tools. These measured dimensions were presented and discussed earlier under the subsection entitled Panel Specimens. All dimensions except bead radius were found to be very close to the design values. The bead radius was found to be smaller than the design value near the crown, while increasing to a value considerably larger than the design value adjacent to the flats, i.e., near the panel midplane. This variation in bead curvature suggests that the panels would be stronger than predicted in bending because compression stresses are highest near the crown where the curvature is greatest and much lower near the panel midplane where the curvature is less. However, in the case of pure axial compression, as in the test of specimen 2-R-E-1-C, the compression stress is essentially uniform over the entire cross section and the lesser curvature near the midplane causes the local buckling strength to be less than predicted.

3) Although shear stresses are also essentially uniform over the panel cross section, shear buckle wave lengths are considerably greater than for compression buckles. The good correlation in shear indicates that the local buckling strength in shear is influenced more by the

greater curvature near the crown than by the lesser curvature near the flats. This reasoning accounts, at least partially, for the greater than predicted shear strength observed in testing specimen 2-R-E-2-S.

To assist in predicting test loads and panel behavior for the type 2 panels designed and fabricated in this program, it is suggested that an additional knockdown factor of .86 be applied to the compression local buckling stress as given by equation 14-3 of reference 8. This modification achieves correlation of analysis and test for specimen 2-R-E-1-C, and thus accounts for the variations in bead curvature which resulted from chem-milling after forming. No modification to the local buckling analyses for bending or for shear are recommended. There is not sufficient test data available here to warrant adoption of less conservative analysis methods than those already established by test in reference 8.

The test results from the type 2A specimens confirm what was found in tests of similar aluminum specimens and panels---that is, present analysis methods do not give reliable strength predictions for the fluted tubular panels. This unpredictable behavior is apparently caused by tube distortional modes which were observed and discussed in reference 8. The correlation factors given in figure 32 for these specimens are worse than those obtained from tests of similar aluminum panels. Apparently the presence of end closures at one end of the René specimens allows greater flexibility for distortional modes to develop than in the case of the aluminum local buckling specimens, which were potted at both ends. Some success in reducing the effect of distortional modes was achieved with aluminum panels by using tube stabilizer inserts (see refs. 8 and 9). However, the expected performance and efficiency of the fluted tubular panels were never fully realized, and no satisfactory test/analysis correlation was achieved.

Because a satisfactory analysis for the fluted tubular panels was not achieved, it was decided not to fabricate any 43 in. x 19 in. (109 cm x 48 cm) René panels of the type 2A configuration. Lack of reliable test load predictions could lead to inadvertent panel failure while testing, with resultant damage to the hypersonic wing test structure.

Predicted Panel Strengths for Proposed Test Load Conditions

A proposed test program for the 43 in. x 19 in. (109 cm x 48 cm) René panels fabricated during this program calls for nondestructive testing at elevated temperature with five different load conditions. These conditions will be applied through a built-up wing structure using a whiffle tree to adjust the loading to achieve compression only, shear only, and three different ratios of combined compression and shear. Predicted failure loads for the five proposed test load conditions, with no pressure loading and with p = 0.75 psi (5.2 kN/m^2), and for the design load condition which includes lateral pressure, have been calculated using both the analysis of reference 8 and the analysis modified as suggested in the preceding subsection of this report. These predicted failure loads are for a temperature of 1350°F (1005 K) and are given in table 1. Local buckling is the predicted mode of failure in compression only and in the design load condition. In the other load conditions panel instability is critical when p = 0, and local buckling is critical when p = 0.75 psi (5.2 kN/m^2). In all cases both the local buckling failure loads and the panel instability failure loads are given in the table for reference.

Table 1: PREDICTED FAILURE LOADS FOR CIRCULAR TUBULAR RENE' 41 PANELS AT 1350° F (1005 K)

LOAD CONDITION	PREDICTED FAILURE LOADS – lb/in (kN/m)							
	ANALYSIS OF REFERENCE 8				MODIFIED ANALYSIS			
	p = 0		p = 0.75 psi (5.2 kN/m^2)		p = 0		p = 0.75 psi (5.2 kN/m^2)	
	N_x	N_{xy}	N_x	N_{xy}	N_x	N_{xy}	N_x	N_{xy}
a. N_x ONLY	1224 (214)*	0	875 (153)*	0	1206 (211)*	0	853 (149)*	0
	1252 (219)**		1024 (179)**		1252 (219)**		1024 (179)**	
b. N_{xy} ONLY	0	621 (109)**	0	581 (102)*	0	621 (109)**	0	581 (102)*
		639 (112)*		621 (109)**		639 (112)*		621 (109)**
c. $N_{xy} = 1/4N_x$	1111 (195) **	278 (48.7)	830 (145) *	207 (36.3)	1111 (195) **	278 (48.7)	800 (140) *	200 (35.0)
	1156 (202) *	289 (50.6)	976 (171) **	244 (42.7)	1118 (196) *	279 (48.9)	976 (171) **	244 (42.7)
d. $N_{xy} = 1/2N_x$	805 (141) **	403 (70.6)	690 (121) *	345 (60.4)	805 (141) **	403 (70.6)	666 (117) *	333 (58.3)
	902 (158) *	451 (79.0)	804 (141) **	402 (70.4)	870 (152) *	435 (76.2)	804 (141) **	402 (70.4)
e. $N_{xy} = 2N_x$	278(48.7) **	556 (97.4)	260 (45.5) *	519 (90.9)	278 (48.7) **	556 (97.4)	257 (45.0) *	512 (89.7)
	296 (51.8) *	591 (104)	278 (48.7) **	556 (97.4)	293 (51.3) *	584 (102)	278 (48.7) **	556 (97.4)
f. $N_{xy} = 0.3125N_x$ (DESIGN CONDITION)	——	——	800 (140) *	250 (43.8)	——	——	770 (135) *	240 (42.0)
			946 (166) **	296 (51.8)			946 (166) **	296 (51.8)

* LOCAL BUCKLING FAILURE

** PANEL INSTABILITY FAILURE

CONCLUSIONS

The objectives of this program were to extend the advanced structural panel technology developed with aluminum (see refs. 6-10) to a superalloy material, specifically René 41, and to produce panels which will be tested at high temperature to evaluate their performance in a typical hypersonic airframe application. These objectives have been met. Satisfactory fabrication methods for producing these panels in René 41 were developed and are documented in this report. Six specimens of these panels were fabricated and delivered to the Flight Research Center where they will replace selected beaded panels in the existing hypersonic wing test structure (see reference 11) and will be tested under combined loads of compression and shear at 1350°F (1005K).

Evaluation of panel performance is deferred until after the elevated temperature tests have been completed. However, room temperature tests of smaller specimens have demonstrated that the end closure designs and the fabrication methods employed result in adequate strength to transmit panel design and test loads into the panel specimens. Local buckling strength of these specimens in axial compression was found to be less than predicted because of deviations in the bead radii from the design value. This deviation causes a predicted strength reduction in the design load condition of three percent. With no lateral pressure applied the predicted strength in axial compression loading is reduced by only two percent, and predicted panel strengths in the other proposed test load conditions are unaffected, since panel general instability is the predicted mode of failure in these cases. With a lateral pressure of 0.75 psi (5.2 kN/m^2) the predicted strengths in the proposed test load conditions is no greater than 3.5 percent.

Specific recommendations regarding the design and manufacture of these panels in René 41 are made as follows:

1) The joint mass penalty for the René 41 panels is 36% which is twice that found for similar aluminum panels in reference 8. This higher joint mass penalty can be attributed to excess doubler mass. The doublers were made thicker than necessary for strength in order

to be compatible with the existing hypersonic test structure and beaded panels. By optimizing the design of the doublers specifically for the tubular panels, the joint mass penalty could be reduced considerably.

2) Multiple-sheet stack-ups cause difficult resistance welding problems. Doublers should be formed from a single sheet of adequate thickness and chem-milled as necessary to obtain reduced thickness transitions.

3) Additional end closure development is warranted. Variations in configuration and forming sequence should be investigated to eliminate compression wrinkling during end closure forming.

4) Closer thickness control would result in better panel cross section configuration control by eliminating the need for chem-milling to obtain the desired sheet thickness. For production quantities, final panel sheet thickness should be negotiated with the supplying mill.

REFERENCES

1. Shideler, John L. and Jackson, L. Robert, "Fuselage and Tank Structure for Hypersonic Aircraft," Conference on Hypersonic Aircraft Technology, Ames Research Center, Moffett Field, CA NASA SP-148, May 1967.

2. Anderson, Melvin S.; Robinson, James C.; and Klich, George F., "Analysis of Wing Structures for Hypersonic Aircraft," Conference on Hypersonic Aircraft Technology, Ames Research Center, Moffett Field, CA, NASA SP-148, May 1967.

3. Plank, P. P.; Sakata, I. F.; Davis, G. W.; and Richie, C. C., "Hypersonic Cruise Vehicle Wing Structure Evaluation," NASA CR 1568, May 1970.

4. Card, M. F.; Davis, J. G.; and Shideler, John L., "Advanced Design Concepts for Shuttle Airframe Structures," NASA Space Shuttle Technology Conference, San Antonio, TX, April 12-14, 1972, NASA TM X-2570, July 1972.

5. Shideler, John L.; Anderson, Melvin S.; and Jackson, L. Robert, "Optimum Mass-Strength Analysis for Orthotropic Ring-Stiffened Cylinder Under Axial Compression," NASA TN D-6772, July 1972.

6. Musgrove, Max D.; Greene, Bruce E.; Shideler, John L.; and Bohon, Herman L., "Advanced Beaded and Tubular Structural Panels," J. of Aircraft, Vol. 11, No. 2, February 1974.

7. Musgrove, M. D. and Greene, B. E., "Advanced Beaded and Tubular Structural Panels," NASA CR-2514.

8. Greene, Bruce E., "Advanced Beaded and Tubular Structural Panels," Substantiation data for, Volume 1, Design and Analysis, NASA CR-132460.

9. Musgrove, Max D. and Northrop, Russell F., "Advanced Beaded and Tubular Structural Panels," Substantiation data for, Volume 2, Fabrication, NASA CR-132482.

10. Hedges, Philip C. and Greene, Bruce E., "Advanced Beaded and Tubular Structural Panels," Substantiation data for, Volume 3, Testing, NASA CR-132515.

11. Plank, P. P. and Penning, F. A., "Hypersonic Wing Test Structure Design, Analysis, and Fabrication," NASA CR-127490, August 1973.

NASA CR-132646

DISTRIBUTION LIST
NAS1-10749

	No. Copies
NASA Langley Research Center **Hampton, VA 23665**	
Attn: Report & Manuscript Control Office, Mail Stop 180A	1
Technology Utilization Office, Mail Stop 139A	1
Roger A. Anderson, Mail Stop 188	1
Robert W. Leonard, Mail Stop 188	1
Dr. Michael F. Card, Mail Stop 190	1
Dr. Martin Martin M. Mikulas, Jr., Mail Stop 190	1
Dr. Paul A. Cooper, Mail Stop 208	1
Dr. Melvin S. Anderson, Mail Stop 190	1
Dr. Jerry G. Williams, Mail Stop 245	1
James C. Robinson, Mail Stop 208	1
Herman L. Bohon, Mail Stop 208	1
Dr. Sidney C. Dixon, Mail Stop 208	1
Harvey G. McComb, Jr., Mail Stop 362	1
James P. Peterson, Mail Stop 245	1
H. Neale Kelly, Mail Stop 208	1
L. Robert Jackson, Mail Stop 160B	1
John L. Shideler, Mail Stop 208	15
NASA Ames Research Center **Moffett Field, CA 94035**	
Attn: Library, Mail Stop 202-3	1
NASA Flight Research Center **P. O. Box 273** **Edwards, CA 93523**	
Attn: Library	1
Roger A. Fields	1
NASA Goddard Space Flight Center **Greenbelt, MD 20771**	
Attn: Library	1
NASA Lyndon B. Johnson Space Center **2101 Webster Seabrook Road** **Houston, TX 77058**	
Attn: JM6/Library	1
Jet Propulsion Laboratory **4800 Oak Grove Drive** **Pasadena, CA 91103**	
Attn: Library, Mail 111-113	1
NASA Lewis Research Center **21000 Brookpark Road** **Cleveland, OH 44135**	
Attn: Library, Mail Stop 60-3	1

NASA CR-132646

DISTRIBUTION LIST

NAS1-10749

	No. Copies
NASA John F. Kennedy Space Center Kennedy Space Center, FL 32899 Attn: Library, IS-DOC-1L	1
NASA Marshall Space Flight Center Huntsville, AL 35812 Attn: AS61L/Library EH/41/William A. Wilson	1 1
National Aeronautics & Space Administration Washington, DC 20546 Attn: KSS-10/Library RW/NASA Headquarters	1 1
McDonnell Douglas Corporation Post Office Box 516 St. Louis, MO 63166 Attn: L. C. Koch, Mail Stop 152	1
AVCO Corporation Aerostructures Division Nashville, TN 37202	1
Bell Aerosystems Company Box 1 Buffalo, NY 14205	1
Bell Helicopter Company P. O. Box 482 Fort Worth, TX 76101	1
General Dynamics Corporation P. O. Box 748 Forth Worth, TX 86101	1
General Dynamics Corporation Convair Division P. O. Box 1128 San Diego, CA 92112	1
Grumman Aerospace Corporation South Oyster Bay Road Bethpage, NY 11714	1
Republic Aviation Corporation Farmingdale, NY 11735	1
Lockheed Aircraft Corporation P. O. Box 504 Sunnyvale, CA 94086	1

NASA CR-132646

DISTRIBUTION LIST
NAS1-10749

	No. Copies
Lockheed Aircraft Corporation 2555 North Hollywood Boulevard Burbank, CA 91504	1
Lockheed Aircraft Corporation Lockheed-Georgia Company 86 South Cobb Drive Marietta, GA 30060	1
LTV Aerospace Corporation Grand Prairie, TX 75050	1
McDonnell Douglas Corporation 3855 Lakewood Boulevard Long Beach, CA 90801	1
McDonnell Douglas Corporation 5301 Bolsa Avenue Huntington Beach, CA 92647	1
McDonnell Douglas Corporation P. O. Box 516 St. Louis, MO 63166	2
Martin Marietta Corporation The Martin Company Post Office Box 179 Denver, CO 80201	1
Rockwell International Corporation Los Angeles Aircraft Division International Airport Los Angeles, CA 90009	1
Rockwell International Corporation 12214 Lakewood Boulevard Downey, CA 90241	1
United Aircraft Corporation Sikorsky Helicopter Stratford, CT 06602	1
Kaman Corporation Old Windsor Road Bloomfield, CT 06002	1
Northrop Corporation 1001 E/ Broadway Hawthorne, CA 90250	1
General Electric Company Valley Forge, PA 19481	1

NASA CR-132646

DISTRIBUTION LIST
NAS1-10749

	No. Copies
Air Force Flight Dynamics Laboratory Wright-Patterson Air Force Base, OH 45433	1
Rohr Corporation P. O. Box 878 Chula Vista, CA 92010	1
Rohr Corporation 620 East 111th Place Los Angeles, CA 90059	1
Rohr Corporation P. O. Box 643 Riverside, CA 92502	1
NASA Scientific & Technical Information Facility 6571 Elkridge Landing Road Linthicum Heights, MD 21090	30 plus reproducible